ΠΑΝΕΠΙΣΤΗΜΙΟ ΑΙΓΑΙΟΥ – ΣΧΟΛΗ ΠΕΡΙΒΑΛΛΟΝΤΟΣ – ΤΜΗΜΑ ΕΠΙΣΤΗΜΩΝ ΤΗΣ ΘΑΛΑΣΣΑΣ

Plastic Litter Project 2020: requirements and design of a marine debris remote sensing calibration/validation campaign.

Δημήτρης Παπαγεωργίου

ΔΙΠΛΩΜΑΤΙΚΗ ΕΡΓΑΣΙΑ

Επιβλέπων Καθηγητής: Κωνσταντίνος Τοπουζέλης

Μυτιλήνη, Φεβρουάριος 2020

ΔΙΠΛΩΜΑΤΙΚΗ ΕΡΓΑΣΙΑ

Αποφοίτου του ΠΜΣ Ολοκληρωμένη Διαχείριση Παράκτιων Περιοχών

Δημήτρη Παπαγεωργίου

ΑΝΤΙΚΕΙΜΕΝΟ ΕΡΓΑΣΙΑΣ:

PLASTIC LITTER PROJECT 2020: REQUIREMENTS AND DESIGN OF A MARINE DEBRIS REMOTE SENSING CALIBRATION/VALIDATION CAMPAIGN

Τριμελής Επιτροπή Επίβλεψης και Κρίσης της Εργασίας	Υπογραφές
Τοπουζέλης Κωνσταντίνος	
Κρασακοπούλου Ευαγγελία	
Ζερβάκης Βασίλης	

Ευχαριστίες

Ευχαριστώ θερμά τον κύριο Τοπουζέλη για την ευκαιρία να συμμετέχω ενεργά στην υλοποίηση του PLP 2019 και τον σχεδιασμό των επόμενων πειραμάτων, καθώς και την συνεχή καθοδήγηση και εμπιστοσύνη του. Ταυτόχρονα, ευχαριστώ θερμά όλους με όσους δουλέψαμε μαζί την άνοιξη του 2019 για την πολύ όμορφη συνεργασία, και ελπίζω να συνεργαστούμε και πάλι στο επόμενο Plastic Litter Project.

Περίληψη

Τα θαλάσσια πλαστικά απορρίματα (ΘΠΑ) αποτελούν ένα σύγχρονο περιβαλλοντικό και οικονομικό πρόβλημα παγκόσμιας σημασίας, η κλίμακα του οποίου μόλις πρόσφατα έχει αρχίσει να εκτιμάται. Η παρακολούθηση των παγκόσμιων συγκεντρώσεων επιπλέοντων θαλάσσιων απορριμάτων είναι αναγκαία για την αντιμετώπιση του προβλήματος και η δορυφορική τηλεπισκόπηση είναι αυτή τη στιγμή πιθανότατα η πιο υποσχόμενη μέθοδος για συστηματικές παρατηρήσεις παγκόσμιας κλίμακας. Η παρούσα μελέτη περιγράφει τις προδιαγραφές και το σχεδιασμό των πειραματικών διαδικασιών για τη λήψη τηλεπισκοπικών δεδομένων επιπλέοντων τεχνητών στόχων με θαλάσσια πλαστικά απορρίματα υπό ρεαλιστικές συνθήκες (PLP2020), με σκοπό τη δημιουργία μιας ανοιχτής βάσης δεδομένων φασματικών υπογραφών ΘΠΑ, η οποία θα χρησιμοποιηθεί για την αναπτυξη ενός ολοκληρωμένου συστήματος παρακολούθησης θαλάσσιων απορριμάτων.

Abstract

Anthropogenic marine debris is a contemporary environmental and economic issue of global importance, the scale of which has only recently begun to be evaluated. The systematic observation of global concentrations of floating marine debris is required for effective mitigation, and satellite remote sensing appears to date the most applicable method for robust systematic monitoring of global scale. The present study details the requirements and design of a floating marine debris remote sensing data acquisition campaign in realistic conditions (PLP2020), for calibration and validation purposes of marine debris detection algorithms and the compilation of a shareable spectral library of characteristic floating marine debris, to be used towards the development of an integrated marine debris observing system (IMDOS).

Contents

1. Introduction

The term plastic encompasses a variety of synthetic and semisynthetic organic materials, almost exclusively polymers with high molecular weight (Tokiwa et al, 2009). Bakelite, the first fully synthetic plastic was manufactured in 1907 (Baekeland, 1909), but widespread production did not occur before the Second World War. Plastic is now produced at an increasing rate, with production reaching 64.4 million tonnes (Mt) in Europe and 348 globally for 2017, with the largest market sector being packaging (PlasticsEurope, 2018), making it one of the most used materials. Lightweight, cheap, durable and with a variety of other desirable properties, plastics are found in countless applications. It is plastics' abundance and durability however, combined with lack of appropriate end-of-life management that presents a great issue concerning the natural environment and especially marine ecosystems, along with billions in cleanup costs, damage to sea vessels and loss of revenue from tourism and fisheries (Gold et al, 2013). As of 2015, only 9% out of the total of 6300 metric tons of plastic waste generated was recycled, 12% incinerated and 79% disposed of in land-fills or accumulated in the natural environment (Geyer, Jambeck & Law, 2017).

With current recycling rates for plastic being about 14-18% out of 302 Mt per year waste produced at the global level, much lower than those of other widely used materials like industrial metals and paper, and incineration at 24%, about 58-62% of all plastic waste produced is disposed of in landfill or the natural environment (Geyer, Jambeck & Law, 2017). Plastic recycling rates differ significantly within the globe, different waste streams and polymers, with some polymer types being more widely recycled than others- polyethylene terephthalate (PET) and high-density polyethylene (HDPE) commonly exceeding 10%, while polystyrene (PS) and polypropylene (PP) are closer to zero (OECD, 2018).

Most megacities are located in the coastal zone (Brown et al, 2013), with around 40% of the world's population living in areas no more than 100 km away from sea (UN, 2017). In Europe, more than 40% live in areas 50 km or less from the ocean and the trend is rising (EUROSTAT, 2017). High population density in coastal areas translates to high plastic waste generation. It is estimated that between 4.8 and 12.7 Mt entered the ocean in 2010, about 8.3 Mt per year, which is projected to double by 2025 (Jambeck et al, 2015). Mismanaged waste, that is waste that is littered or inadequately disposed uncontained in dumps or open, uncontrolled landfills, can enter the ocean through river or wastewater outflows and transport by wind, tides and currents (Jambeck et al, 2015). Among the average of 8 Mt of the total plastic waste entering the ocean in 2010, the plastic input due to river transport, is evaluated between 1.15 and 2.41 Mt of plastics every year, corresponding to 9-50% of total plastic transport to the ocean (Lebreton et al., 2017). Once in the ocean, plastics can float on or just below the surface or sink to the bottom, depending on the specific polymer's molecular weight. PET or polyvinyl chloride (PVC) for example with densities above that of seawater will eventually sink, while PS or HDPE will generally float. Biofouling, the formation of an organic biofilm due to life processes on the surface of both macro and microplastics, can cause plastic debris that would otherwise float on the surface to sink to the bottom, or oscillate vertically (Kooi et al, 2017). About 60% of plastic produced floats, as it is less dense than seawater (Andrady, 2011). Marine debris that floats, either of natural or anthropogenic origin, tends to be trapped in subtropical gyres – large systems of circular ocean currents (Goldstein and Goodwin, 2013), or is recaptured by coastlines (Kako et al, 2014). The Great Pacific Garbage Patch (GPGP) is one of such accumulation zones for buoyant plastic that has been identified in the North Pacific Subtropical Gyre (Wong, Green & Cretney, 1974). A recent study (Lebreton et al, 2018) showed that the GPGP is increasing exponentially in size and at a faster rate than the surrounding waters, while over 75% of its mass is attributed to debris larger than 5mm and more than 46% is thought to be comprised of fishing nets. The Mediterranean along with the Black Sea, harboring large coastal populations, have inevitably also been found to contain large concentrations of floating marine plastics, with accumulations comparable to those of the great ocean gyres (Van Sebille et al, 2015; Suaria & Aliani, 2014; Suaria & Aliani, 2015; Cozar et al, 2015; Suaria et al, 2016). Suaria and Aliani (2014) found that in the Mediterranean basin, 78% of all sighted objects were of anthropogenic origin-95.6% of which was plastic, with highest concentrations in the Adriatic Sea and Algerian Basin and lowest in the Central Tyrrhenian and Sicilian Sea, while calculating that more than 63 million macroplastic items are currently floating on the surface of the Mediterranean basin.

Plastics do not readily biodegrade, persist in the environment and are of great concern due to their effects on the marine environment, wildlife and potentially humans (Thompson, 2009). Whether floating on the surface, suspended in the water column or sunk to the bottom of the ocean floor, marine plastics pose great environmental, ecological, economic and possibly health implications, a fact illustrated by the increasing amount of peer reviewed publications being published yearly (Thevenon et al, 2014). Effects of plastic debris on marine life are well documented throughout the scientific literature. More than 267 marine species are known to have been affected by marine plastics, either by ingestion – which affects mostly marine birds, or entanglement – which affects mostly marine mammals (Hammer, Kraak & Parsons, 2012). Lost or discarded fishing nets – ghost nets, are also very problematic as marine species continue to be trapped for many years – ghost fishing (Matsuoka et al, 2005). Studies have also shown that various fish species around the world are ingesting microplastics in a regular basis (Lusher, McHugh & Thompson, 2013; Neves et al, 2015). A meta-analysis of controlled experimental studies showed possible negative effects of plastic ingestion on zooplankton and fish species, including reduced consumption of natural prey, along with negative effects on growth, reproduction and survival (Foley et al, 2018). Besides posing a risk due to mechanical implications in the digestive tracks of marine animals, plastics readily absorb or adsorb other potentially harmful organic compounds and metals present in seawater (Lee et al, 2014; Homes et al, 2012), acting as vectors for bioaccumulation for these substances (Ziccardi et al, 2016). In addition, plastics have also been found to leach out additives which act as endocrine disruptors to marine life (Chen et al, 2019). There has been increased concern on the implications for human health, although research on potential adverse effects from consumption of seafood affected by marine plastics or direct human ingestion of microplastic particles is currently lacking (Lusher et al, 2017). Although the lack of data, potential mechanisms for microplastics to impact human health have been identified (Wright and Kelly, 2017). Coupled with potential health implications for humans, concentrations of microplastics detected in seafood can seriously endanger the food security of many areas and translate into great economic losses (Gallo et al, 2018). Fish and other seafood play a determining role in the diet of millions of people, especially in developing coastal areas, with billions in annual revenues (FAO, 2016). High macroplastic debris concentrations have been reported to greatly impact subsistence fishermen in Indonesia as early as 1992 (Nash, 1992). Including effects to tourism and recreation, global marine plastic contamination has been estimated to account for an annual loss of $0.5 to $2.5 trillion in the value of benefits derived from marine ecosystem services (Beaumont et al, 2019).The cost to the environment and marine life, potential cost to human health, along with the implicated economic costs, all serve as an urgent call to action in order to curb the severe issue of marine plastics.

Anthropogenic marine debris has been identified as a major quality descriptor by the MSFD and significant efforts are being targeted towards the establishment of general guidelines for the monitoring of marine litter (MSFD, 2013; GESAMP, 2019). Efforts in the detection of marine plastic while still on the ocean surface have mostly targeted at predicting concentration zones and transport patterns using modelling approaches of physical parameters and data from drifters, as well as in situ observations (Critchel and Lambrechts, 2016; Mansui et al, 2015; Lebreton et al, 2012; Maximenko et al, 2011; Law et al, 2010), however present ocean circulation models are not yet able to accurately simulate debris drift (Maximenko et al, 2019). Detection of marine plastics through remote sensing applications is an emerging field and so far no integrated method exists to effectively detect marine plastic debris on the ocean surface using publicly available satellite imagery. A recent White Paper publication (Maximenko et al, 2019) presented the concept of an Integrated Marine Debris Observing System (IMDOS). The IMDOS, based largely on the GOOS program, will combine remote sensing (various platforms and sensor types) and in situ data to provide global coverage and accuracy, for the monitoring of marine debris, understanding of distribution dynamics and evaluation of mitigation efforts; in addition providing accurate estimates of variables required for the SDG 14.1 indicators under development by UNEP (GESAMP, 2019). In order to provide data for calibration and validation processes of satellite sensors and detection methodologies, series of repeated ground-thruthed in situ observations are needed. These in situ observations will assists in answering vital questions such as: what is the minimum detectable subpixel abundance of plastic debris, is it possible to distinguish between different polymer types in floating marine plastic, what are the best atmospheric and sunglint correction methodologies for marine debris detection, what is the relationship between the degree of submersion and the reflectance properties of plastics, among others. However, in order to become useful, the in situ observations need to be compiled as spectral measurements in large spectral libraries of different types of debris (Maximenko et al, 2019). The Plastic Litter Project (PLP) 2020, building on the experience gained from PLP 2018 and 2019, will primarily aim to contribute towards the creation of a shareable, multi-sensor and multi-instrument spectral library of floating marine debris signatures in near-real environmental conditions, to be used towards the development of marine litter detection methodologies and an integrated marine debris observing system. The present study details the project requirements, design and expected outcomes for the

Plastic Litter Project 2020, which will be conducted by the Marine Remote Sensing Group at the University of the Aegean in Lesvos.

2. Remote sensing of marine plastic debris

In the past years, an increasing amount of studies have focused on the remote detection of floating marine plastic debris using airborne sensors; most focus on hyperspectral imaging. The spectral properties of hydrocarbons (plastics are essentially hydrocarbons), mainly their characteristic absorption features, have long been examined for remote sensing applications (Cloutis, 1989). During the 1990's at least two studies focused on the use of multispectral Landsat Thematic Mapper (TM) and Daedalus data to detect hydrocarbons (Bannert et al, 1994; Kühn and Hörig, 1995), but the spectral resolution of both sensors was not high enough to distinguish hydrocarbons using subtle absorption features that can be detected with field spectroscopy (Hörig et al, 2001). More recent studies have focused specifically on floating marine debris, with advancements in sensor technology allowing for higher spatial and temporal resolution data acquisition.

Garaba and Dierssen (2018) used a PANanalytical ASD FieldSpec 4 spectrometer to measure the spectral reflectance of wet and dry microplastics harvested from the North Atlantic Ocean, macroplastics washed ashore and virgin plastic pellets in a range of 350 to 2500 nm; their signatures were compared and quantified in order to evaluate the feasibility of plastic debris optical remote sensing. They identified prominent absorption features in the NIR and SWIR ranges – specifically at ~931, 1215, 1417 and 1732 nm (fig.1), consistent along the different objects analyzed.

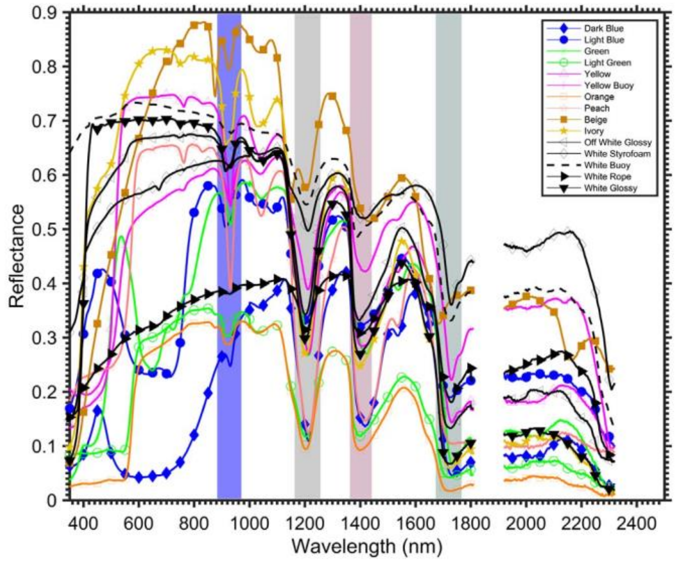

Figure 1: Reflectance of macroplastics showing apparent absorption features in NIR and SWIR ranges (Source: Garaba and Dierssen, 2018)

The dry microplastic reflectance spectra could be represented as a single bulk average signature, that when compared to reference signatures of dry virgin pellets showed moderate similarity to common plastics, consistent with what is reported globally for microplastic composition of marine debris. Macroplastics had discreet signatures that were not bulked into a single average as they were not necessarily representative of the composition of floating plastic debris. The wetness factor was found to diminish the overall magnitude of the signal, but the spectral shape was not affected. Due to absorption features of the atmosphere – mainly water, the 1215 and 1732 nm absorption bands were found to be applicable through an intervening atmosphere. These were used in a modified algorithm from Kühn et al. (2004) to map plastic concentrations in and around the area of a landfill (in absence of aquatic scenes), using airborne visible-infrared imaging spectrometer (AVIRIS) hyperspectral imagery. The HI index from Kühn et al. (2004) was modified to match the channels of the AVIRIS spectrometer.

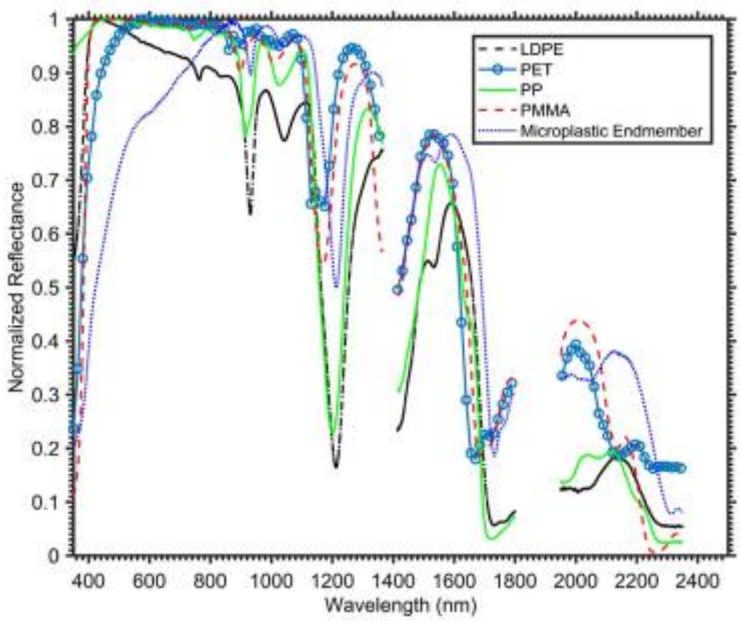

Figure 2: Normalised reflectance of microplastic bulk and virgin pellets, showing charcteristic absorption features (Source: Garaba and Diersse, 20018)

In further work, Garaba et al. (2018) used a SASI-600 Imager (950 to 2450 nm) onboard a C-130 aircraft to capture images in the area of the Great Pacific Garbage Patch (GPGP). Very high resolution RGB images were also captured and georeferenced on top of SWIR images, allowing for detailed ocean plastic identification from trained observers. Their analysis focused on a large ghost net, where a distinct floating part could be identified. They performed spectral shape comparison of identified plastics with spectral signatures of known polymer types from a previously compiled spectral library (Garaba and Dierssen, 2018) using spectral contrast angle calculations. Finally they applied and assessed the applicability of HIs previously developed. The SWIR signal of the ocean plastics identified was in general consistent among ocean plastic types with small variations. They identified several absorption features, the common absorption features around 1215 and 1732 nm being of most interest. The polymer composition of the ghost net could not be effectively identified comparing its spectral signature to that of know polymer types from the spectral library. Results from spectral unmixing simulations suggest that the aforementioned absorption features have potential for detecting ocean plastics using SWIR sensors. A decrease in the pixel coverage with plastic results in a decrease in the band depth at each absorption feature. They conclude that a simplified quantification and detection algorithm based on a band depth method requiring a minimum of three wavebands, including the absorption waveband, can be used for both distinct features.

In a similar approach, Acuña-Ruz et al (2018) performed a supervised classification of marine debris on beaches, using very high resolution WorldView 3 (WV3) images and hyperspectral signatures from a series of spectrometers. They collected macroplastic (>25mm) debris from a series of beaches in the Chiloé Island region of Chile, which were spectraly analyzed using three different hyperspectral spectrometer systems (HyLogger 3 reflectance spectrometer, PS-300 Apogee and ASD Field Spec) in the 380 to 2500 nm range. The spectral signatures were then filtered for outliers (standard deviation) and compiled into a reference spectral library (fig. 3). The hyperspectral signatures were convolved to correspond to the spectral bands of the WorldView 3 satellite sensor using RSRCalculator (Duran-Alarcon et al, 2014). The Spectral Ampitude Difference metric (Feret and Asner, 2011) was used in order to evaluate spectral separability between the different class signatures.

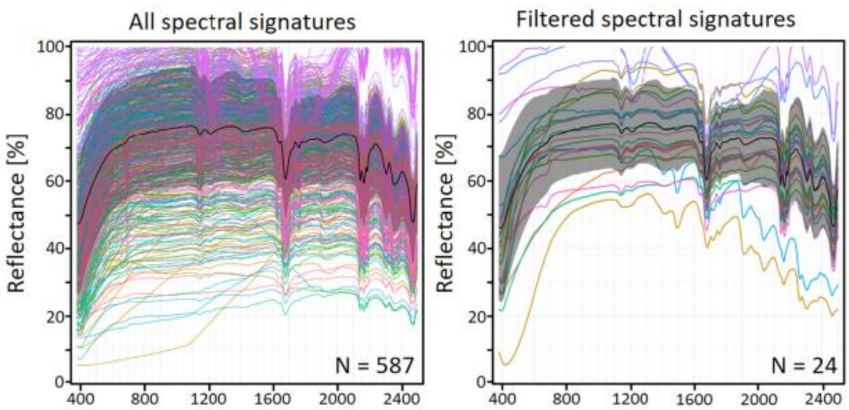

Figure 3: Spectral signatures acquired by HyLogger 3, showing characteristic absorption bands (Source: Acuña-Ruz, 2018)

In order to develop a supervised classification model, 90 pixels from each class (expanded polystyrene (EP) and other plastics) were selected from the scene. The convolved spectral signatures from WV3 were used to train non-parametric methods such as Support Vector Machine (SVM) and Random Forest (RF), which do not assume any representative statistical distribution of training data and often have greater classification power with small data sets. The built database was separated into one subset for training (70%) and another for validation. As with previous studies, characteristic absorption features were identified in the 1670-1690 nm, 2130-2190 nm and 2430-2500 nm regions. EP had a unique spectral characteristic that allowed separability from the other debris and so 2 classified categories were established: EP and Mixture. All supervised classification methods performed with accuracies >75%, with radial SVM classification performing better overall with accuracies close to 90%. Inclusion of other spectral bands could enable the distinction between other types of plastics besides EP.

Goddijn-Murphy et al. (2018) developed a model to explain light reflectance of buoyant plastics on water, based on geometrical optics and the spectral signatures of plasic and seawater, which takes into account the colour, transparency, reflectivity and shape of marine plastics. They took into account the different ways plastics floating on water affect surface leaving reflectance in nadir view – light reflects directly off plastic than water, light transmittance through plastic is different through the water-air interface changing backscattering and subsurface upwelling light. Allowing for a number of approximations (a single smooth flat layer of plastic with specific physical and optical properties, bi-directionality of plastic reflectance of sunlight, shading and filtering of downwelling light by plastic on the surface) and given a known reflectance of the clear sea surface and that of plastic, the fraction of plastic surface area can be estimated. In a following work Goddijn-Murphy and Dufaur (2018) presented a proof of concept of the reflectance model for macroplastics under an experimental setup (fig. 4).EPS foam, HDPE and PET bottle reflectances were measured using the Analytical Spectral Devices FieldSpec Pro hyperspectral instrument (350 – 2500 nm). Spectral coefficients of diffuse reflectance, total reflectance, transmittance and absorption of the target materials were also measured in the laboratory using the same instrument. They point out that in the case of plastic bottles, two parallel surfaces of plastic interacting with light instead of one, given a nadir reflectance measure can be described as the sum of reflectance form top and bottom layers. Due to the refractive index of water being higher than air and closer to HDPE and PET, reflectance of a semi-transparent layer of plastic is expected to be lower than r – reflectance it would have in air, and that of two layers higher than r but lower than r2, but the effect was not present in field measurements.

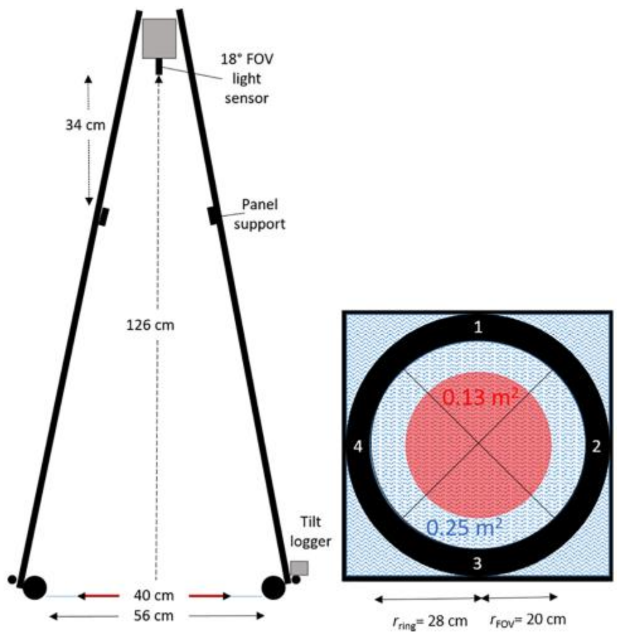

Figure 4: Experimental setup showing the floating frame; diameter field of view in red; side and plan views (Source: Goddijn-Murphy and Dufaur, 2018)

EPS foam was found to have the greatest overall reflectance throughout the spectrum, followed by HDPE and PET, while all materials presented a characteristic absorption band at around 1680, 1730 and 1660 nm respectively, especially prevalent in PET. The effect of size of litter on reflectance was investigated using two different sizes of bottles, and results suggested that larger bottles are better reflectors. The model is designed to work with any wavelength and 850 nm was used in the single band process, with regression analysis showing highly significant regressions in support of the reflectance model. Field measurements of reflectance could not be satisfactorily calculated using reflectance coefficients derived from laboratory measurements. The results also showed no evidence of a shading effect. The dual band process was evaluated using 850 nm as λ_1 – where reflectance of plastics is high and outside the visible range of the spectrum, and λ_2 was set at the absorption bands observed in the laboratory measurements. The two wavelengths were selected also for the reflectance of water being the same in both bands and close to zero. While $\Delta\rho_p$ is highest for each plastic when its specific absorption band is used, the PET absorption band was also used for all three types of plastic to evaluate the use of a common λ_2. However assigning λ_2 at the PET absorption band $\Delta\rho_p$ for EPS and HDPE was higher than for PET, perhaps due to PET's overall lowest reflectance. In general, reflectance of plastics floating on the surface in natural daylight did no strongly correspond with the reflectance coefficients of the materials obtained in the laboratory. The type of polymer, transparency, shape and surface roughness of the plastic object were determining factors in the relationship between measured reflectance and plastic surface fraction and as a result no general remote sensing algorithm to estimate surface fraction of plastic litter floating on the surface of natural waters is proposed.

In a first large scale approach towards a remote sensing application for the detection of floating marine debris, Topouzelis et al. (2018), with the assistance of University of the Aegean students and researchers, conducted an experiment in which they constructed 3 10x10m targets out of PET, LDPE blue plastic bags and nylon fishing nets (all supported by a plastic mesh), which were deployed at sea and anchored at about 30 m offshore from Tsamakia beach in Mytilene, Lesvos on 07/06/2018. The targets were set floating above *Posidonia oceanica* patches to provide a dark background in an effort to simulate open ocean optical properties (close to zero NIR and SWIR reflectance) (fig. 5). Weather condition were optimal; clear skies, very calm sea with no white caps (1-2cm waves) and low wind speed (2 m/s). A series of imaging systems onboard a S900 DJI hexacopter were used to acquire very high resolution RGB images (Sony A5100), 4-band multispectral images (450, 500, 550 and 850 nm from a Slantrange 3P; 550, 660, 735 and 790nm from a Parrot Sequoia) and high resolution thermal images (FliR DUO R) of the scene. In addition, the experiment was timed to coincide with acquisition times of the Sentinel 2 (S2), WV3 and PlanetScope (PS) satellites, each one acquiring an image of the scene while the targets were deployed. The high resolution RGB images form the A5100 were processed using the structure from motion photogrammetric pipeline algorithm for orthophoto production. All high resolution images including the S2 satellite image were georeferenced using the orthophoto map produced.

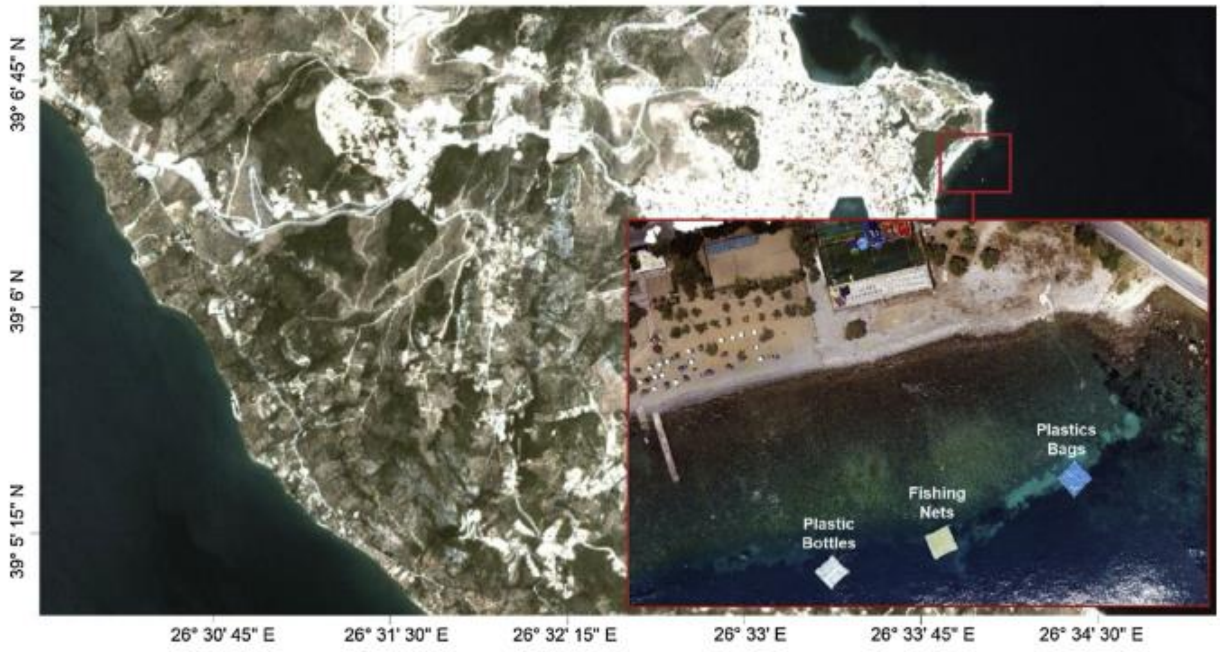

Figure 5: RGB from a PlanetDove image and Sony A5100 showing the three targets floating off Tsamakia beach (Source: Topouzelis et al, 2018).

Percentage pixel coverage for each of the target pixels was evaluated using the very high resolution A5100 orthophoto, which was used as a master image to improve georeferencing of the S2 image (fig. 6). All 10x10 m targets were readily distinguishable in the 10 m resolution bands of S2; with the exception of the blue bag targets that were not easily distinguishable in the green and red bands (fig. 7), providing evidence for potential applications of the S2 satellite in detecting floating marine debris.

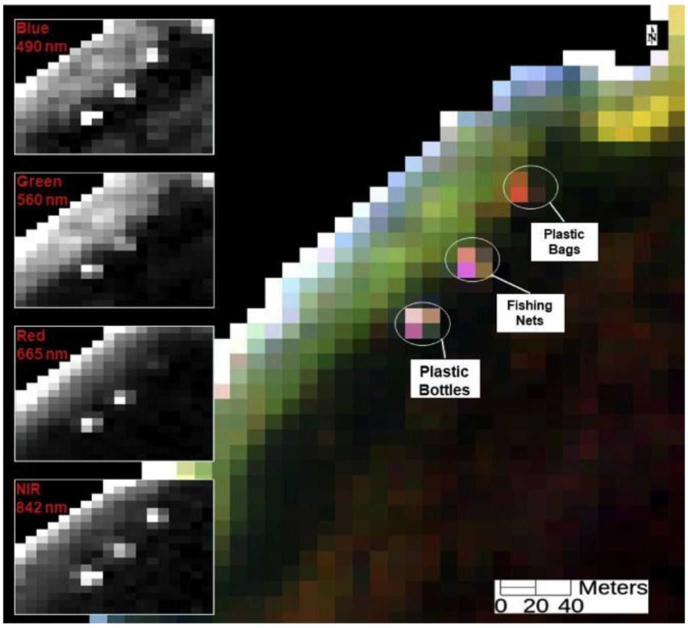

Figure 6: RGB composite and RGB and NIR greyscales of target area (Source: Topouzelis et al, 2018)

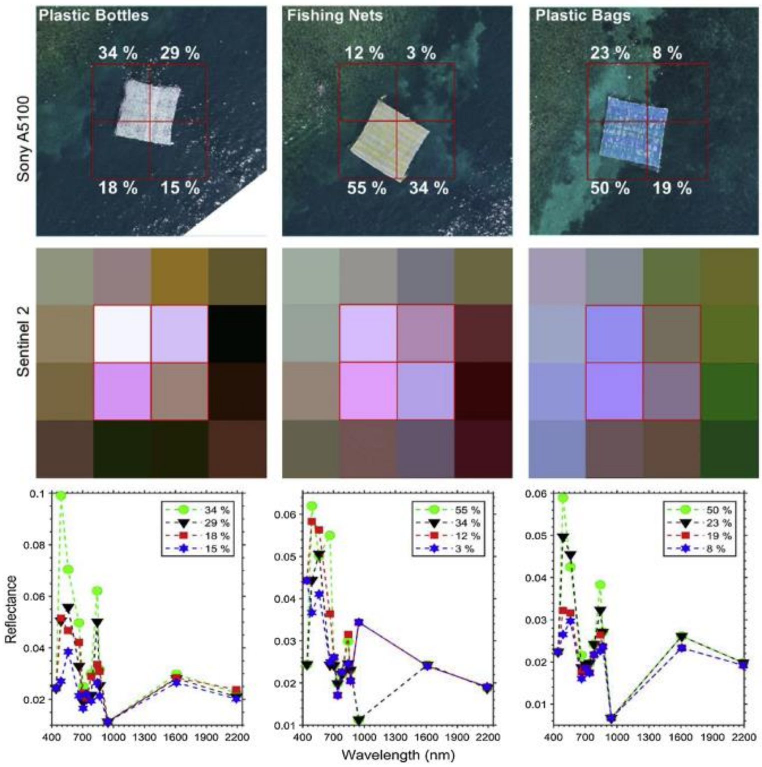

Figure 7: Pixel coverage and S2 signatures – left to right: PET bottles, fishing nets, LDPE plastic bags (Source: Topouzelis et al, 2018)

From April to June 2019, a second experiment was performed by the University of Aegean Marine Remote Sensing Group (MRSG) with the participation of a number of Marine Sciences students. The experiment was a follow-up of the 2018 PLP and involved the construction of a number of plastic and natural debris targets that were deployed at sea off Tsamakia beach. The targets were constructed of a rectangular 5x5 m frame made from PVC ø 2.5 cm pipes. The frame was fastened on a 5x5 m plastic mesh 1.4 cm in hole size to create a base on which the target material would be supported. As in PLP 2018, two holes were drilled in the bottom and the cap of the bottles and fishing line was threaded through to create a line of 16 bottles, with tags removed. The blue plastic LDPE bags were threaded onto the plastic mesh with fishing line. The natural debris targets were constructed using reeds. Reeds are very plentiful in Mediterranean coastal ecosystems and are a common constituent of natural debris floating on the sea surface (Suaria et al, 2015); as such they were deemed suitable for the approximation of non-anthropogenic marine debris in this study. The reeds were gathered from nearby locations, cut to length and left to dry, in order to avoid any photosynthetically active material remaining in leaves. The reeds were then weaved together using thin nylon rope into 2.5x2.5 m "quadrants" that were connected to the 5x5 m frame. The targets and quadrants were possible to connect in a modular fashion to create different configurations of target material. In total 5 different S2 images were acquired with the targets in various configurations. The plastic cover area of the targets was also modified throughout the experiment. In the case of plastic bags target, part of the sheet of plastic mesh with the attached bags was removed from the frame. For the plastic bottle targets the mesh was not removed as the bottles would fill up with water while floating, risking cutting the fishing line and breaking the frame while removal of the targets from the water. In addition to the S2 data, several high resolution RGB reference images were acquired using a DJI Phantom drone.

Initial processing and analysis (not presented here) of these *is situ* data by both MRSG and other institutions and researchers, has provided valuable insight into the possible methodologies to be used for marine debris detection using various remote sensing platforms, as well as the factors affecting the marine debris signal and thus the detection capabilities. Spectral unmixing calculations have indicated the possibility to use such algorithms for the detection and quantification of floating marine debris, but a pure pixel signature of various marine debris scenarios is needed in order to be able to produce the most valuable results. In addition, novel indices and those used for the detection of floating *Sargassum* macroalgae are also under investigation.

A recent publication by Martinez-Vicente et al. (2019), tying into the proposed IMDOS, outlines an initial assessment of observation requirements for monitoring marine plastic debris form space. They tackle both floating marine plastic and over land observations, and identify a series of scientific questions to be answered in terms of marine debris in general and challenges to be met in terms of defining the characteristics of a marine debris remote sensing system.

The *in situ* data and resulting spectral libraries acquired from experimental campaigns such as the PLPs will assist greatly in the development and calibration of marine debris detection missions and methodologies. The main issues that the PLP2020, and following projects, will aim to help resolve are:

- what is the minimum detectable subpixel abundance of plastic debris, based on current mission sensors spatial and spectral resolutions and SNRs,
- is it possible to distinguish between different polymer types in floating marine plastic
- what are the best atmospheric and sunglint correction methodologies for marine debris detection
- what is the relationship between the degree of submersion and the reflectance properties of plastics
- what is a reasonable SNR for spectroradiometric detection of marine plastic debris
- to what extent can spectral unmixing algorithms be used for marine debris quantification

3. Plastic Litter Project 2020 – requirements and design

In order for the acquired data to be useful in terms of a spectral debris library they need to fulfill a set of requirements. Since there are no specific guidelines when it comes to a large-scale project of this kind, these requirements are formulated based on prior experience with PLP 2018 and 2019, experience gained through working with marine debris remote sensing data, as well as through communication with experts in the field of marine debris and the relevant literature. The main identified requirements are as follows:

1) The target materials need to consist of characteristic marine plastic debris polymers or natural debris – this is to ensure that the acquired data and spectral signatures will be representative of floating marine debris

in waters around the world, so that they are specifically relevant in terms of an integrated marine debris observing system.

2) The target materials need to include representative natural debris, characteristic of the area of application (such as *Arundo donax* reeds, wood and marine vegetation), in mixed target scenarios and/or pure natural debris targets– this is needed in order to investigate the capacity to discriminate between natural marine debris and that of anthropogenic origin.

3) Any water leaving reflectance not attributed to the target materials (bottom reflection, suspended matter etc.) needs to be minimized or accounted for – this will ensure that the acquired spectral measurements are free of signal contribution from non-target sources.

4) At least one target needs to be of sufficient area in order to guarantee a full 10x10m pixel coverage, independent of target orientation in the image matrix – a “pure” marine debris signature can be readily and more accurately used in spectral unmixing algorithms, to investigate the capacity of marine debris quantification

5) Data acquisition from non-satellite platforms (UAS, hand held spectrometer), including metadata, needs to be concise, timely and robust – this is to ensure that all data are intercomparable

6) The targets must be straight-forward and relatively easy to construct, deploy and repair – this will ensure project realization and allow for better management

7) The target design must ensure that no anthropogenic marine debris is lost to the environment

8) The design of the project and targets must ensure that the process is repeatable and applicable to different locations, in order to contribute towards the establishment of best practices in terms of marine debris remote sensing validation and calibration campaigns.

3.1 Polymeric composition and characteristics of marine plastic debris

In order for the target materials to be representative of floating marine plastic debris in nature, it is important that the polymeric composition of the targets matches that of what is observed in coastal and open ocean waters. As previously stated, the Mediterranean has been found to contain concentrations of floating marine debris similar to those of the great oceanic gyres. Although most polymeric composition studies on floating marine debris focus on microplastics, all secondary microplastics are produced through degradation and as such can be thought of as characteristic of the overall polymeric composition of larger floating marine plastic debris. In general, high density (HDPE) and low density polyethylene (LDPE), along with polypropylene (PP), regardless of size of the object, are found to dominate the surface of ocean and coastal waters around the world, as well as the world’s beaches, while most macrolitter items consist of packaging and single use items (UNEP, 2015; Suaria et al, 2016; Pasternak et al, 2017; Munari et al, 2017; Baini et al, 2018; Brignac et al, 2019, among others). Other floating polymers such as polystyrene

(PS) and polyacrylics (PA) are also present in surface waters but in lower concentrations. One of the biggest sources of HDPE in the ocean are ghost nets, which are thought to account for almost half of the mass of the GPGP (Lebreton et al, 2018). Although in general HDPE and LDPE are found in greater concentrations in ocean waters and on beaches, studies have also found that expanded polystyrene foam products (EPS) can also be found in increased concentrations in both surface waters and beaches (Suaria and Aliani, 2014; Brignac et al, 2019).

Marine plastic debris, although comprising the majority of floating debris, are many times found floating in amalgamations with natural debris. Specific to the Mediterranean, Suaria and Aliani (2014) found a positive correlation between the abundance of anthropogenic and natural marine debris, indicating that on a larger scale, the two types of debris tend to accumulate in the same regions, with 22% of all sighted objects during their transects being of natural origin. Most floating macrolitter tends to be less than 50cm in size (Suaria and Aliani, 2014; Brignac et al, 2019), with the exception of large ghost nets and EPS foam objects (Lebreton et al, 2018; Garaba et al, 2018; UNEP, 2015). Suaria and Aliani (2014) found that 57.8% of all sighted plastic objects were between 10 and 50cm in length, 35% were <10cm and 7.2% were >50cm; while 31% of EPS foam objects were entire fish boxes of around 60-70 cm in length, with 31% being fragments between 10-50 cm and 41% <10cm. In terms of density, mean marine debris concentrations in the Mediterranean for macrolitter items have been found to range from less than 2.5 items/km^2 (McCoy, 1988; Topcu et al, 2010; UNEP/MAP/MEDPOL, 2009), to 15-25 items/km^2 (Alliani et al, 2003) and 24.9 items/km^2 (Suaria and Aliani, 2014), with peak conncentrations reaching above 54 items/km^2. These concentrations, comparable to what is observed in the ocean gyres, are in no way detectable by available satellite sensors. The constantly increasing amounts of marine plastic pollution however, in combination with extreme events, will most likely result to future concentrations being detectable by space.

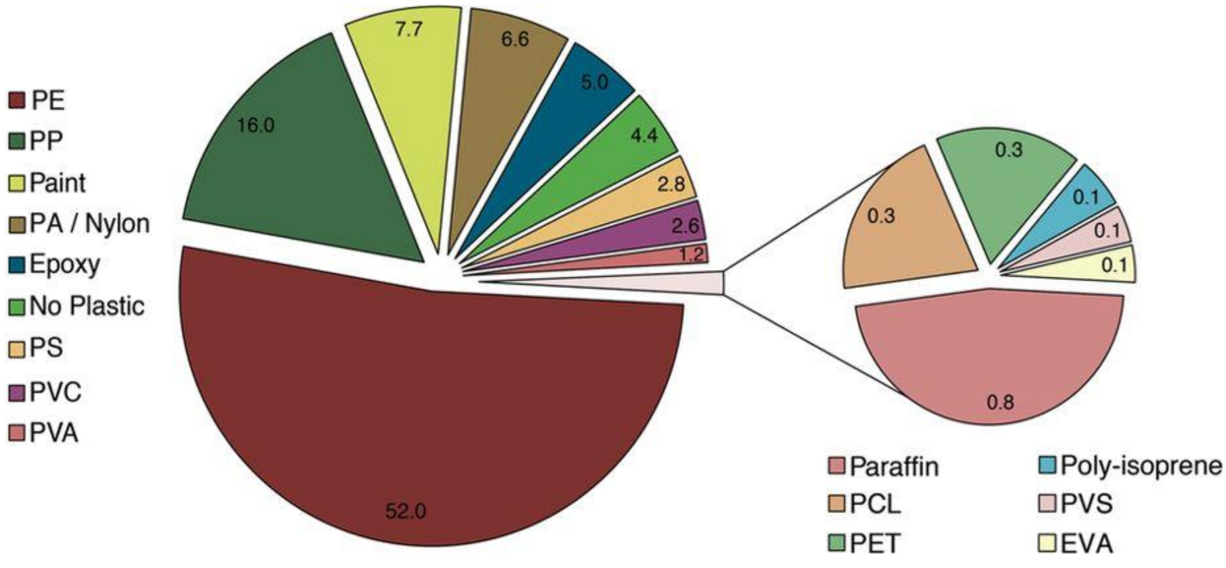

Figure 8: Polymeric composition of particles in Mediterranean surface waters (Source: Suaria et al, 2016)

3.2 Target materials – characterization of marine plastic debris

The target materials will consist of representative marine plastic debris objects and polymers, that will be collected during a series of beach cleanings which will be performed early spring in the island of Lesvos. Windward beaches have been shown to collect higher densities of marine debris (Moy et al, 2018; Brignac et al, 2019). The north eastern Aegean is dominated by prevailing north and north eastern winds. In addition to the fact that the eastern Mediterranean coasts are considered as a significant marine debris input zone, it is expected that beaches in the north and eastern part of the island will have higher concentrations of beached marine debris. It is essential for the beach cleanings to be performed before the start of the touristic and bathing season, since a number of beaches are cleaned for aesthetic purposes.

The survey methodology will follow recommendations found in “Guidelines for the monitoring and assessment of plastic litter in the ocean” (GESAMP, 2019), and collected materials will be sorted and catalogued in terms of size, polymer type (where possible), litter type (where applicable) and auxiliary info such as origin of manufacture (appendix 1). The above report, building on MSFD (2013) and UNEP/IOC (2009), aims to provide recommendations, advice and practical guidance for establishing programmes to monitor and assess the distribution and abundance of plastic litter. For the purposes of PLP2020, only macroplastic items larger than 5 cm in the longest dimension will be considered for use as target materials. The rest of the gathered materials will be stored for possible further sorting and analysis, or disposed of responsibly. All candidate items will be sorted and stored in separate categories/containers based on size and polymer composition (Annex 2). In essence, the collected marine debris will be divided in two main categories based on size: those between 5 and 10 cm in the longest dimension, and those ≥ 10 cm. These two categories will be subdivided based on polymer composition, as shown in the cataloguing form in Annex 2. A further subdivision based on litter type might be applicable, but this is to be decided based on the results of the first beach cleanings. All items with unknown polymer composition will be tested for positive buoyancy in containers filled with seawater, to exclude items that have a higher density than seawater and may not have come from the sea. Based on the polymeric composition of marine plastics discussed above, polymers that will be used as target materials will be: HDPE and LDPE (which will be treated generically as PE), PP, PS, EPS foam, as well as PET. The main litter types will most likely consist of single use items – bottles, food containers, plastic bags, foam products, along with crates, fishing gear, ropes and nets. Although PET is a sinking polymer and PET litter will eventually sink to the sea bottom, PET bottles and cups are commonly sighted floating on the sea surface of busy coastal waters and as such are considered suitable as a target material.

Due to the fact that it is not possible to accurately estimate the amount of material that will be needed for the targets, nor the amount of plastic debris that will be collected during the beach cleanings, it is not possible to determine whether the collected debris will be enough to cover the intended area of the targets. In this case, alternative sources of target materials need to be established. For 2018 and 2019 the PET bottles for the targets were collected locally through a citizen network, this can be repeated for typical items such as HDPE bottles and packaging.

In addition, several groups and organisations in Greece perform regular beach cleanings that could provide part of the target materials.

The natural debris to be used as target materials will also be collected during the beach cleanings. In addition, as in PLP 2019, Arundo donax reeds, a characteristic species of coastal vegetation abundant in Mediterranean transitional ecosystems and river basins that is a common constituent of floating marine debris, will also be used as target materials of natural origin. The reeds will be cut to length and dried in order to avoid any photosynthetically active materials remaining in the vegetation.

The exact polymer ratios that will be used for the target materials will be mainly decided by the amount of each polymer that will be collected during the beach cleanings. However, as a general rule, based on what is reported for floating and beached debris, the polymer and debris type concentrations will be: 30% PE, 20% PP, 10% PS, 10% EPS and 10% PET packaging and single use items, along with 20% items of varying use and polymer type – mostly dominated by PE. In the case of the larger semi-permanent targets, debris types will also include large fishing nets – mostly PE, larger EPS pieces and larger floating debris in general. For the mixed targets, a general ratio of 60% anthropogenic to 40% natural debris will be used. It is important to note that these ratios are in no way exact or universally applicable, since there is great temporal and spatial variation in the amounts reported in the literature, but are however considered adequately representative as an initial approach that is subject to reconsideration.

3.3 Target design and development

Two types of targets will be constructed for PLP 2020:

1) <u>Re-deployable 5x5 m modular targets, based on the design of the targets used for PLP2019:</u>

These will consist of a rectangular frame, constructed with HDPE-100 pipes. HDPE-100 is a floating polymer (density range 950-965 kg/m^3) that is commonly used in low and medium pressure water and gas applications, as well as for the construction of cages in aquaculture applications. HDPE 100 with a long term design stress of 10 MPa, will provide high tensile strength and overall rigidity to the target frames, while retaining the necessary flexibility in order to sustain dynamic loading from deployment and wave action. The higher strength of HDPE compared to PVC will also eliminate the need for cross-bracing the frame as in PLP2018 and 2019. The pipes will be 4 mm in diameter with a wall thickness of 2.4 mm and will be joined using 90^o angle connections. Housings for GPS units will be positioned at two opposing corners of each target frame. Each target frame will weigh less than 7 kg (including GPS housings and connections, excluding target materials).

The target materials will be “woven” into strands of 5 m in length using high-strength fishing line and/or thin floating rope. Only debris ≥ 10 cm will be used for the strands in order to facilitate the woving procedure and reduce the total number of items needed to cover the 25 m^2 target area. Each strand will be populated with items of the same debris type (packaging-bottles, packaging-box etc.) and polymer, in order to allow for a better management of litter type and polymer ratios for the target materials. In addition to plastic items, marine debris of natural origin (such as reeds and driftwood) will also be used to populate the targets. These will be woven together to form surfaces of about 2x5 m, which will be interwoven with the plastic litter strands on the target to form a mixed debris surface. A stainless ring will be tied to the end of each strand in order to facilitate attachment to the target frame. The strands of debris will be interchangeable and replaceable, allowing for target reconfiguration and repair. This will be achieved by a line of rope passing through the rings at the ends of each strand in order to create a canopy-like configuration (fig. 9). Instead of each separate strand being tied to the target frame, the whole canopy will be attached by securing the line of rope along the side of the target frame. Percentage coverage of the targets (area of target covered by debris over total area of target) will be controlled by removing or adding strands on the target frames, as in PLP2019. During the strand production phase, the plastic target materials will be pre-positioned inside the 5x5 m frame to ensure proper area coverage and dispersion of the materials. Every produced strand will be characterized and catalogued using the form in appendix 3.

In addition to allowing the targets to float on the sea surface, it will be possible to slightly raise the target frame from the surface in order to investigate the effect of the wetness factor, which has been shown to reduce the floating debris signal significantly (Garaba et al, 2018). This will be achieved by attaching buoys underneath the target frame, which will rise it from the surface and given a calm sea, will prevent the debris from being wet. The buoys will be painted a matte black colour in order to minimize signal contribution.

A total of 6 5x5 m target frames and the corresponding strands will be aimed to be constructed. This amounts to a total of 150 m^2 of target surface area. This will allow for the modular connection of series of targets to create configurations such as windrows-although in a smaller scale, and provide a robust indication of the minimum detectable abundance fraction of marine debris in a pixel for different imaging platforms. However, the capacity to reach the 6 target threshold will be governed mostly by the number of people involved in the project and the amount of debris that will be collected from all sources.

Target deployment will be performed in the same manner as in PLP2018 and 2019, with a series of teams (at beach, at sea and dinghy) working in tandem to deploy and anchor the targets. The beach team picks up and transports the target frames to the break-wave area, were the sea team joins the target frames to create the desired configuration and delivers the target to the dinghy/divers team which transports the target to the anchoring position and secures the target in place. The anchors are set before the first deployment of the targets and remain at sea with a buoy marker for identification. After data acquisition the process is repeated in reverse; the dingy team unties and returns the target to the sea and beach teams, that remove the target from the water and place it on the beach for storage.

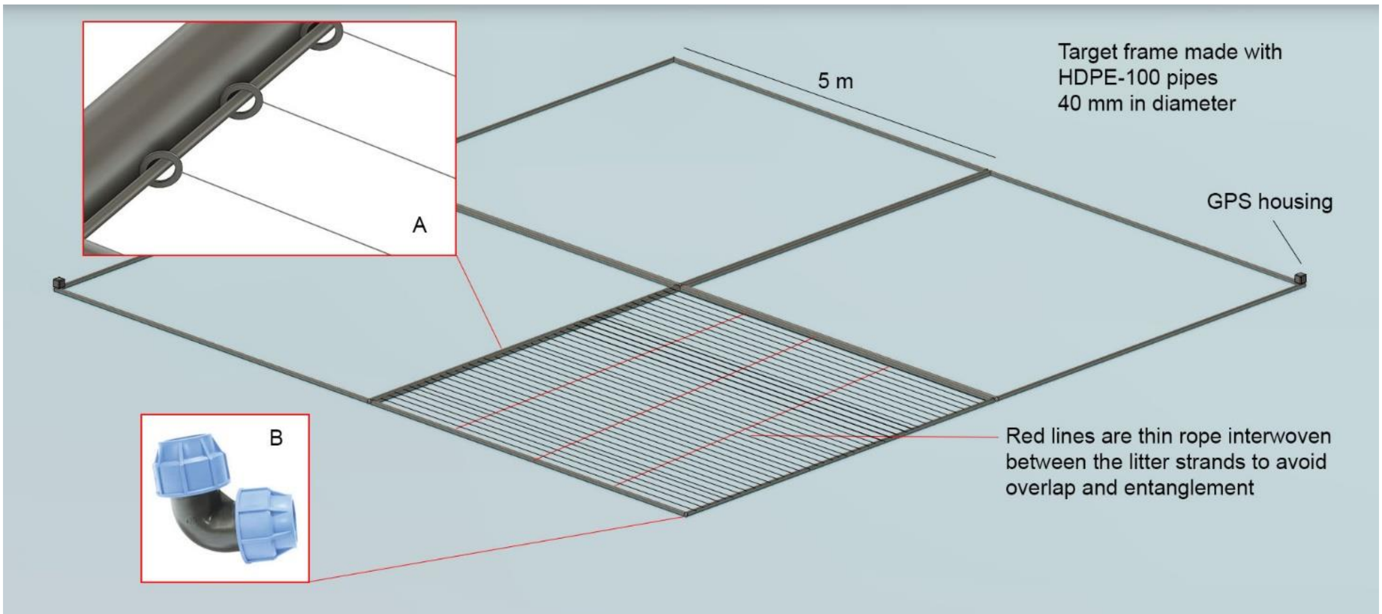

Figure 9: In scale 3d rendering of the modular targets in a 10x10 m square configuration. Cutout A shows the line passing through the strand rings and is attached to the target frame. Cutout B shows the 90° compression fitting. Strand lines are thicker for visualization purposes, target material not shown.

2) Semi-permanent large circular targets:

The aim of these targets is to ensure a full Sentinel 2 (10x10m) pixel coverage by the target area. This will allow for the retrieval of a pure marine debris signature, which can be used effectively in spectral unmixing calculations and index development. Trial and error calculations have shown that in order to ensure full pixel coverage, a circular target needs to be at least 22 m in diameter. A circular configuration is favored against a square one, as at such scales the loading pattern on a square frame due to the wave action could lead to increased stress and deformation. In addition, a circular frame of that size is much easier to construct and allows for a smaller surface area needed to guarantee a full pixel coverage compared to a square target.

The semi-permanent targets will be also constructed with HDPE-100 pipes, and will take the general form of an aquaculture cage. 110 mm diameter HDPE-100 pipes, with a wall thickness of 6.6 mm will be used to construct a 22 m diameter ring. A pressure fitted connection will be used to join the two ends of the pipe to create an air-tight ring. This will form the base of the target. A second ring, with a smaller diameter of 63 mm and a wall thickness of 3.8 mm, will also be constructed using HDPE-100 pipes. The two rings will be connected together to form a cylindrical cage structure, using vertical rods spanning 1.5 m from bottom to top ring (fig. 10). The rods will consist of concrete reinforcement steel bars 12 mm in diameter, with a rectangular 15x4 cm, 3 mm thick steel plate welded on both ends. All rods and plates will be painted to avoid major corrosion. The rods, 12 in total at 5.5 m intervals, will be fastened on the pipes by clamping the plates using circular stainless steel pipe clamps (fig. 10). The resulting cylindrical structure will form the target frame, which will be constructed on site and deployed at sea for the duration of the experiment.

The target will be populated with plastic debris ≥ 5 cm, as well as larger debris and bundled fishing nets and natural debris. In order to avoid any loss of material to the environment and facilitate the placement and removal of the material in and from the target, a large closed-loop net will be used. The net will work as an oversized shopping net, closed at one end, and with a line of rope on the other that closes the bag when tightened. The net containing the target materials will be dropped inside the target frame, and the line of rope will be tightened along the circumference of the frame, essentially creating a butterfly net-like type of construction, allowing the target materials to float freely inside the frame. A series of small weights will be attached to the net so that it sinks in place inside the target frame creating a barrier that the debris cannot cross. Each time the target materials need to be removed or replaced, the rope is removed from the frame and tightened to close the net, and the net is lifted from the target frame. The target will be securely anchored to the sea bottom using 3 5 kg ship anchors, which will be set firmly by a diver team and a dinghy at 120° angles between them in a circular pattern around a center point. The three anchors will be attached to the main ring of the target frame and will work in tandem in order to hold the target firmly in place against currents of any direction. The exact radius of the anchor setting pattern will need to be calculated based on the depth of the water column were the target will be deployed, but in general, a scope of at least 1.5:1 will need to be achieved (length of rope from anchor to target= 1.5 x depth of water column).

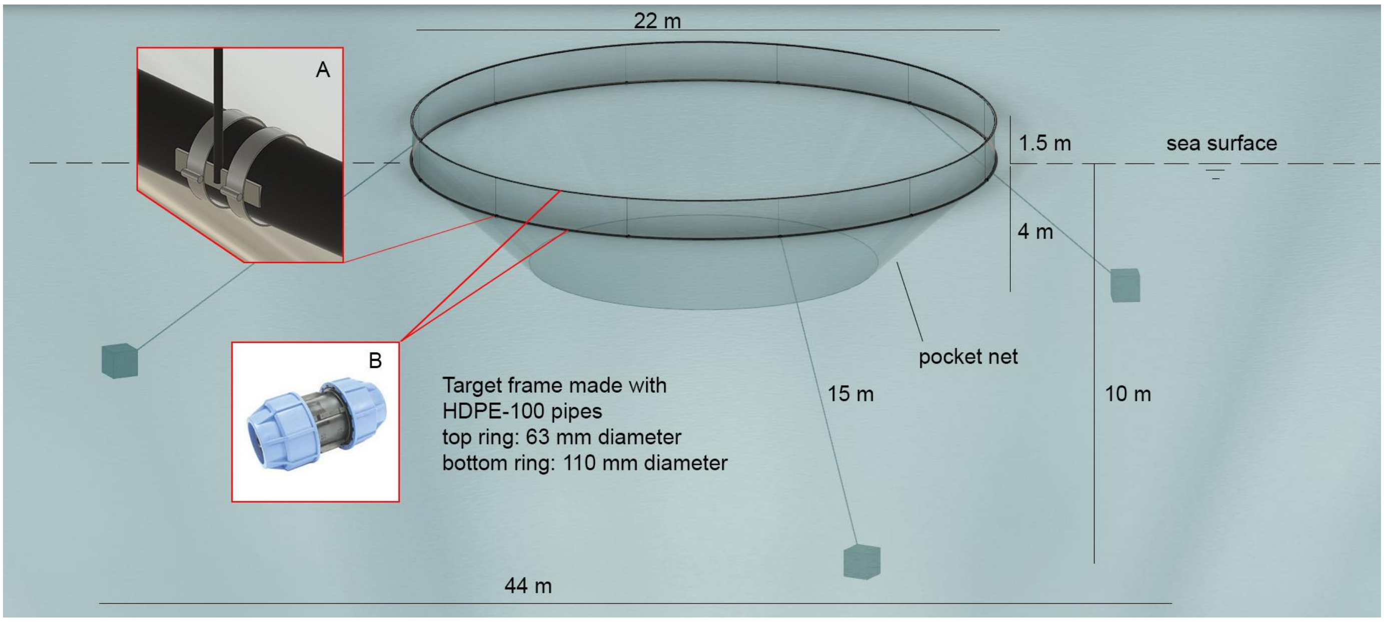

Figure 10: In scale 3D rendering of the semi-permanent circular target. Cut-out A shows the support rod with attached plate connection to the frame using clamps. Cutout B shows the compression type connection that will be used to close the loop of each ring, connecting the two pipe ends together.

This particular target design presents some inherent advantages and disadvantages. The size of the target – 22 m in diameter and approximately 260 kg in total weight, requires assembly on site, increased logistical efforts and a considerable number of people involved in the construction and deployment of the target. The fact that the target will remain deployed at sea for the duration of the experiment means that a license will need to be procured from the local coastal authorities, and the site of deployment must be such that it causes no interference with shipping lines or daily coastal activities. The anchoring of the target to the sea bottom will require the work of a dive team, as well as a dinghy for towing the target and setting the anchors. A dinghy will also need to be used for the deployment and removal of the target materials by use of the containing net. The use of the net to work both as a barrier for the target materials not to escape outside the target frame, as well as a container for the debris to be transported in, eliminates the need for a permanent fixture of the target materials to the target frame. This greatly facilitates the construction and experimental procedure and ensures a more realistic experimental environment, as the target materials will be free-floating inside the target frame. In addition, the size of the target allows for the incorporation of much larger target materials – such as ghost nets, large EPS pieces, bigger containers, that are common constituents of floating marine debris. Since the target materials will be allowed to float freely inside the frame, they will be subject to forces acted upon them from waves, wind and surface currents, and will inevitably start to drift. If the target frame is anchored and not allowed to drift as well, the debris will eventually tend to gather on one edge of the target frame, possibly piling against the frame wall created by the net. This effect will be somewhat mitigated by the fact that the floating bottom ring will reduce the force of waves and surface currents inside of the target frame, while the relatively tightly woven net will produce some wind resistance. However, the gathering of the target materials on the edge of the target frame will likely constrict the conditions under which it will be possible to retrieve robust data. In any case, data acquisition in rougher than calm seas is problematic. The above effect can also further be mitigated if the target is allowed to float freely during data acquisition.

Both the bottom and top rings will inevitably contribute to overall signal. In-situ measurements, along with empty target data acquisitions can be used to assess and mitigate the effect of the rings' reflectance to the overall signal. However, the buoyancy of the bottom ring can be controlled in a way that it is not floating, but suspended in the water column underneath the surface. This can be achieved by the use of a water inlet and outlet valve, which are used to control the amount of seawater inside the bottom ring, in order to reduce its buoyancy and make it possible for it to be held under the surface by the anchor lines.

The magnitude of the target design dictates the need for a small scale prototype to be constructed, in order to test the validity of the design and assess the amount of debris stacking against the target frame. For this reason, 5 m diameter target will be constructed and deployed at sea using the same materials and methodology. This will allow to evaluate and mitigate any design flaws and provide for a proof of concept.

3.4 Site selection

Both PLP2018 and 2019 were conducted in the close vicinity of Tsamakia beach in Mytilene, Lesvos. The close proximity to the city of Mytilene, the available open space, as well as the relative protection offered by the small bay makes this beach ideal for this kind of experiment; at least in terms of the smaller re-deployable targets. The *Posidonia oceanica* patches that exist at about 60 m from the shoreline present an adequately dark substrate, in order to simulate open ocean water reflectance effectively. The intended area of deployment will be sampled using a field spectrometer to identify the ideal positions for the target anchoring. Great care needs to be taken during placement of the anchors, which will be performed by a dive team and not from a dinghy, in order to avoid damage to the *P.oceanica* meadows.

Figure 11: Possible deployment sites in the Gulf of Gera for the large circular target (source: modified from Google Earth images)

Site selection for the bigger semi-permanent targets is inherently more complicated than for the small 5x5 m targets. Tsamakia beach is in general a busy area, with organized beach-going facilities in the vicinity, as well as shipping routes that pass close to the shore. A structure of this size would most likely interfere with everyday activities and it might not be possible to obtain a license for. Several areas inside the gulf of Gera are more suited for the long-term deployment of the large 22 m diameter target (fig. 11). The many small protected coves inside the gulf and the fact that no high waves form in such a small basin, make it an ideal site. The same restrictions apply regarding bottom reflectance, however the depth of the water column has to be sufficient (≥10 m) in order to guaranty robust anchoring of the target. One disadvantage of the gulf of Gera is the increased amounts of suspended matter and optically active constituents in the water column in general, that will affect the overall water leaving reflectance in some degree, differentiating it from that of the open ocean water. However, this can be accounted for and mitigated using in-situ data collected from the field spectrometer, as well as the signal from the surrounding waters. The gulf of Gera, which has relatively low marine traffic, is also ideal for allowing the target to float freely under supervision on the sea surface. The buoyancy and structural integrity of the target frame guaranty that it can be towed safely by a dinghy, allowing for exact positioning or retrieval. In any case, site selection for the large circular target will have to be made in accordance and cooperation with the local authorities.

3.5 Data acquisition and metadata

The main data acquisition schedule will follow the acquisition plans of a series of satellite platforms; mainly the Sentinel 2A and 2B, Sentinel 1, Landsat 8, Worldview III, Planet Scope and PRISMA. The Sentinel 2A and 2B acquisition plan for Europe is such that for any location there is a new image every 5 days – Sentinel 1A and 2B satellites acquire data over Lesvos at about 12:00 local time every 5 days; while for Landsat 8 the revisit time is 16 days. Sentinel 1A and 1B revisit Lesvos with the same orbit every 6 days for 2 consecutive days, resulting in a series of different products for each of the two days (Sentinel 1 is an active radar sensor and as such is capable of night time data acquisition). All Sentinel and Landsat acquisition plans are available in .kml file format through the respective space agencies websites (sentinel.esa.int; landsat.usgs.gov). For Worldview 3 the revisit time is on average less than 1 day at 40^o latitude (Lesvos is 39^o). The same applies for PlanetScope. PRISMA satellite data will also be acquired, but at this stage the satellite acquisition schedule is not known. Table 1 presents a combined acquisition calendar, which will need to be followed strictly to achieve the required data acquisition.

Apart from satellite sensors, a number of other platforms, sensors and instruments will be used for the acquisition of remote sensing data. Unmanned aerial systems (UAS or drones) will be used for the acquisition of very high resolution (VHR) RGB images of the targets during deployment, including the shoreline. These VHR RGB images will be georeferenced using the orthophoto map produced during PLP2018 (Topouzelis et al, 2019) and will be used for the calculation of each target pixel percentage coverage of marine debris in satellite images, as previously done in PLP2018 and 2019. The images will be acquired using an on-board UAS camera or the Sony A5100 RGB camera. In order to ensure minimal errors during the georeferencing process, the acquisition of the images needs to be performed with a nadir-viewing angle, ensuring that the deployed targets, the shoreline and the ground reference points produced during PLP2018, are all included in the image. In addition, if the anchoring of the targets is not such that guaranties no major drifting or rotation, the time of acquisition of the RGB reference images needs to align closely with the acquisition time of the satellite. This is to ensure that the target has not changed position significantly between the two acquisition times, unintentionally resulting in a possibly large error in geolocation. For the larger circular target, in order to calculate the exact percentage coverage that is achieved at the time of data acquisition, VHR RGB images will be used with object based classification algorithms, in the same manner that will be used to calculate the pixel percentage coverage in the satellite images.

In addition to the RGB reference images, all other data acquisitions besides from satellite sensors need to also be concise and robust, in order to guaranty the quality and intercompatibility of the data. Multi-spectral and hyper-spectral data acquisition needs to coincide with satellite acquisition times in order to guaranty identical lighting conditions (sun elevation angles) and a meaningful data comparison. In addition, a constant height of flight and sensor viewing angle, based on manufacturer's recommendations for each sensor, needs to be maintained for all data acquisitions throughout the extent of the experiment. Be more presise about sensors? The same applies for measurements performed using a field spectrometer. All measurements need to coincide with satellite and/or drone acquisition and be performed concisely throughout the extent of the experiment. In-situ measurements will be especially valuable in the evaluation, calibration and improvement of atmospheric and sunglint correction algorithms, tailored to floating marine debris detection.

Metadata collection is an important aspect of general data acquisition, as it ensures knowledge of parameters affecting the quality of the data (e.g. sea surface state, atmospheric conditions, sun elevation angles) and enables the capacity to compare between temporally different data. Most major metadata can be directly and reliably retrieved from satellite products such as Sentinel 2. However, parameters such as sea surface state and wind intensity are important factors that cannot be retrieved reliably from satellite product metadata. A field data and metadata acquisition report is presented in ANNEX 3. Metadata recording will be based on GESAMP (2019) and UNEP/IOC (2009) recommendations, in terms of sea state and atmospheric conditions.

Table 1: Acquisition plans for Sentinel-1, 2 and Landsat 8 satellites

Satellite acquisition plans over Lesvos from 01/04/2020 to 30/06/2020																															
	April																														
	1	2	3	4	5	6	7	8	9	10	11	12	13	14	15	16	17	18	19	20	21	22	23	24	25	26	27	28	29	30	
Sentinel 2		B					A					B					A					B					A				
Landsat 8			■																■												
Sentinel 1		■	■					■	■					■	■					■	■					■	■				
	May																														
	1	2	3	4	5	6	7	8	9	10	11	12	13	14	15	16	17	18	19	20	21	22	23	24	25	26	27	28	29	30	31
Sentinel 2		B					A					B					A					B					A				
Landsat 8					■																■										
Sentinel 1		■	■					■	■					■	■					■	■					■	■				
	June																														
	1	2	3	4	5	6	7	8	9	10	11	12	13	14	15	16	17	18	19	20	21	22	23	24	25	26	27	28	29	30	
Sentinel 2	B					A					B					A					B					A					
Landsat 8						■																■									
Sentinel 1	■	■					■	■					■	■					■	■					■	■				■	

The PLP2020 data acquisition schedule will have to coincide with the data acquisition plans of major satellites that do not have a daily revisit frequency, shown in table 1. The data acquisition schedule will be divided in two main parts, one for each type of target. Characteristic marine debris collected from ocean sources have not been examined in this manner before and in-lack of other in-situ validated data, it is not possible to pre-determine the size or the plastic debris percentage coverage of the targets that will be detectable through the available satellite imagery. The small scale test for the large circular target will most likely provide a good indication, however at this point it is not possible to design a complete and rigid acquisition schedule. Nonetheless, the general acquisition plan is based on the premise that the large full pixel target will provide a pure spectral signature that can be later used with the modular targets, which will provide the basis for evaluating the sub-pixel detection capabilities. The idea is to obtain at least two measurements on different acquisition dates for each target configuration and percent coverage. For a four month period, and 100% acquisition rate, it is possible to retrieve a maximum of 24 Sentinel-2, 6 Landsat-8 and more than 30 Sentinel-1 data acquisitions. However, varying weather conditions and other unforeseen events almost guaranty that the data acquisition rate will be less than nominal. For PLP2019, out of the 13 planned acquisition dates, 5 produced data of sufficient quality, which corresponds to an acquisition rate of about 40%. This amounts to at least 7 S-2 and 2 L-8 expected data acquisitions. The initial acquisition schedule is based mainly on the S-2 satellite, and since there is considerable overlap between S-2 and S-1 acquisition plans, adhering to the S-2 acquisition schedules is sufficient to also obtain S-1 data. The L-8 acquisition schedule is considerably different than that of S-2, with only one overlapping date. Due to the small number and lower rate of L-8 planned acquisitions during the 3 month period, it is not possible to follow a common target configuration plan. For this reason, the PLP2020 L-8 acquisition schedule will aim to obtain at least one image for each of the 2 types modular targets configurations shown in figure 12 at 100% coverage, as well as at least two for the large circular target also at 100% coverage. Configuration type 2 for the modular targets aims to simulate a windrow formation, since windrows have been suggested as potential marine debris concentration zones. Type B configuration for both types will only be used in case type A is not detectable. Target materials for the large circular target will include ghost nets, for which data will be acquired at different acquisition dates.

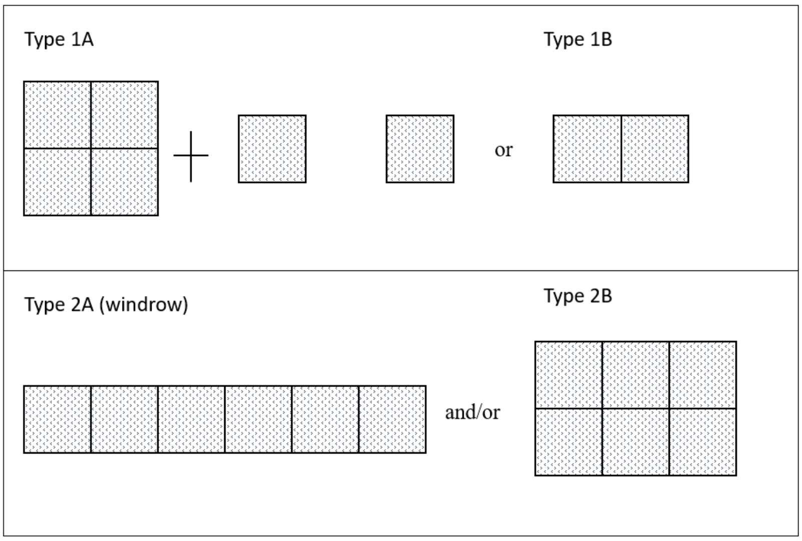

Figure 12: PLP2020 modular targets configuration types; each square is 5x5 m.

The initial acquisition schedule is presented in table 2, superimposed with S-1, S-2 and L-8 acquisition plans. The percentage coverage of the targets is gradually reduced in order to assess the spectral signature variations and minimum detectable concentration of marine debris in a pixel; this will be particularly useful with the larger target that guaranties a full pixel coverage by marine debris. However, the variability of the percentage coverage for the experiment will have to be re-assessed after the first satellite data have been acquired and during the entirety of the data acquisition process. The last two weeks of June have intentionally not been scheduled for data acquisition, to account for any possible delays or alterations to the schedule. This includes possible data acquisitions with free-floating targets and the raising of modular targets above the sea surface to assess for the wetness effect, as well as measurements of targets that have been populated by debris of a single type of polymer, in order to assess the capacity of polymer discrimination. In general, the initial acquisition schedule for PLP2020 acts more as an acquisition requirement guideline, that is open to reassessment after initial data acquisitions.

Table 2: Initial PLP2020 data acquisition schedule, based on Sentinels 2, 1 and Landsat-8 data acquisition plans.

PLP2020 acquisition achedule

April																															
	1	2	3	4	5	6	7	8	9	10	11	12	13	14	15	16	17	18	19	20	21	22	23	24	25	26	27	28	29	30	
Modular targets		1	1				1					2					2		1			1					1				
Circular target		■	■				■					■					G		G			G					G				
Sentinel 2		B					A					B					A					B					A				
Landsat 8			■																■												
Sentinel 1		■	■					■	■					■	■					■	■					■	■				
May																															
	1	2	3	4	5	6	7	8	9	10	11	12	13	14	15	16	17	18	19	20	21	22	23	24	25	26	27	28	29	30	31
Modular targets		2			2		2					1M					1M				1M	2M					2M				
Circular target		■			■		■					■					M				M	M					M				
Sentinel 2		B					A					B					A					B					A				
Landsat 8					■																■										
Sentinel 1		■	■					■	■					■	■					■	■					■	■				
June																															
	1	2	3	4	5	6	7	8	9	10	11	12	13	14	15	16	17	18	19	20	21	22	23	24	25	26	27	28	29	30	
Modular targets	1					1					2					2															
Circular target	■					■					■					■															
Sentinel 2	B					A					B					A					B					A					
Landsat 8						■																■									
Sentinel 1	■	■					■	■					■	■					■	■					■	■				■	

Modular targets:	1 :Type 1A	Circular target:	M :mixed materials	Both types:	:100% coverage
	2 :Type 2A		G :ghost nets & large marine debris		:75% coverage
	1M :Type 1A, mixed materials				:50% coverage
	2M :Type 2A, mixed materials				

3.6 Logistics and management

The Plastic Litter Project 2020 is based on the experience gained from the two previous projects, however some aspects such as target materials and target design and deployment, make PLP2020 an inherently more demanding endeavor in terms of management and logistics. Project management and organization will be performed by the Marine Remote Sensing Group (MRSG) at the University of the Aegean, with an allocated project manager responsible for the general realization of the experiment. Any willing individual can volunteer to participate in PLP2020, but the majority of people involved will be students from the Department of Marine Sciences in UAegean.

In order to facilitate the project management and task allocation, PLP2020 is divided in two main phases: phase one is the pre-data acquisition phase, which includes the beach cleanings, sorting and cataloguing of the materials, circular target small scale prototype testing and target construction and testing; phase two is the main data acquisition phase of the experiment, which includes deployment of the targets, data acquisition and in general all main field activities, including removal, disassembly and storage of the targets and target materials. In both phases, all participants will be allocated to core teams, each responsible for a specific area of activities (dive team, dinghy team, drone team etc.). Table 3 presents a layout and Gantt chart of the main activities in each of the two phases of the experiment, while the task and team organization is presented in table 3 (team organization form in appendix 4).

Table 3: PLP2020 main activities Gantt chart

Plastic Litter Project 2020 main activities layout and Gantt chart																	
	Month	1				2				3				4			
	Week	1	2	3	4	5	6	7	8	9	10	11	12	13	14	15	16
Phase 1	Beach cleanings	■	■														
	Litter cataloguing	■	■														
	Large target prototype	■															
	Target construction	■	■	■	■												
	Target testing				■												
Phase 2	Data acquisition					■	■	■	■	■	■	■	■	■	■	■	■
	Target removal and storage																■
	Site restoration																■

Step one of phase one is to perform the beach cleanings and the sorting and categorization of the collected materials. This task will be performed by the entirety of the people involved with the project. One person (“organizer”) will be responsible for general logistical and managerial aspects of the task, such as participants, logistics and transportation, open call for volunteers etc. Two people (“field managers”) will be responsible for the overall organization and management of the field activities, including necessary equipment (gloves, bags, etc.), field briefings and general safety. Sorting of the collected debris will be carried out at UAegean grounds, which will be stored into containers sorted based on debris size, litter and polymer type. Three task managers will be mainly responsible for the cataloguing of the collected marine debris using the form in appendix 2.

A construction team will be responsible for the assembly of the target frames and production of the litter strands. The main team will be split into two smaller teams, one responsible for the smaller 5x5 m targets and one for the larger circular target. Each team will have a team leader, with a general team manager responsible for all operations. The production of the litter strands is a significantly laborious task, as has been made evident through the 2 previous PLPs, and as such calls for at least 10 people being occupied at all times.

Table 4: Main project tasks and corresponding task teams.

	Tasks	Teams
Phase 1	Beach cleanings	all
	Litter cataloguing	all
	Large target prototype	construction team
	Target construction	construction team; all
	Target testing	beach, dive, dinghy, construction teams
Phase 2	Data acquisition and fieldwork	beach, dive, dinghy, drone, data management teams
	Target dissasembly and storage	construction team; all
	Site restoration	all

During the main phase of the experiment, a number of teams are going to be working in tandem. Experience with PLPs 2018 and 2019 has shown that specific field teams, tasked with a single area of the experiment work best. Two field managers (at least one present at all times during field experiments) will be responsible for the general management and safety of all field related work, and will be the ones that fill out the field reports (appendix 5). A beach team will be responsible for all ground related target activities, moving the target to and from the breakwater and delivering to dive or dinghy team, modifying and repairing the targets. A dive team will be responsible with anything target related in the water (anchors and anchoring of the target, setting of buoys, in-water repairs etc.), along with general in-water management and safety. The dinghy team is the one responsible for operation of the small inflatable boat, which will be mainly used for towing the targets and transporting the target materials to and from the large circular target. A drone team will be responsible for all UAS data acquisition, while a data management team will be responsible for the downloading, quality inspection and initial archiving of all acquired data sets. Briefing of all teams will fall under the project manager's responsibilities, with regular meetings between the team leaders taking place in timely fashion.

4. Outcome and expected results

The main outcome of PLP2020 will be the production of a shareable remote sensing database, containing multi- and hyper-spectral data of floating marine debris targets in realistic conditions, acquired from various satellite, airborne and field sensors and instruments, that will contribute to further development of marine debris spectral libraries and the establishment of an integrated marine debris observing system (IMDOS). The uncertainty regarding marine debris circulation and concentrations, along with insufficient satellite coverage, lack of concurrent in-situ observations, are some of the factors contributing to the very limited number of satellite images confirmed to contain floating marine debris of anthropogenic origin. An in-situ validated, floating marine debris image database of characteristic polymers is an essential tool to be used towards achieving operational global remote sensing monitoring capabilities.

The development of a concise and straight-forward experimental methodology, including experimental requirements and target design, as well as data acquisition, is an essential step towards the establishment of best practices for future marine debris detection calibration/validation campaigns using artificial floating marine debris targets. Best practice methodologies allow for the replication of the experiment by different individuals, regardless of spatial or temporal variability, in a manner that takes into account the same parameters and influencing factors. Essentially, best practices ensure that data and metadata retrieved from different sources – following the same experimental methodologies, are accurate, robust and readily intercompatible.

Besides the remote sensing data, a series of auxiliary datasets will be acquired; among others: marine debris concentration and composition of the beaches that will be cleaned, spatial and/or temporal variability of marine debris concentrations, windward v. leeward concentrations, origin of marine debris. This data while not directly relevant to the remote sensing detection and monitoring of marine debris, is very valuable in terms of better understanding marine debris circulation, origin and sources, as well as for the monitoring of the levels of marine debris pollution on the island of Lesvos, and mitigation efforts against a major anthropogenic issue of global scale.

References

A.L. Lusher, M. McHugh, R.C. Thompson, Occurrence of microplastics in the gastrointestinal tract of pelagic and demersal fish from the English Channel, Marine Pollution Bulletin, Volume 67, Issues 1–2, 2013, Pages 94-99, ISSN 0025-326X, https://doi.org/10.1016/j.marpolbul.2012.11.028.

Adams, J.B., Smith, M.O., Johnson, P.E., 1986. Spectral mixture modeling: a new analysis of rock and soil types at the Viking Lander 1 Site. J. Geophys. Res. Solid Earth 91, 8098–8112. http://dx.doi.org/10.1029/JB091iB08p08098.

Andrady Anthony L. (2011) Microplastics in the marine environment, Marine Pollution Bulletin, Volume 62, Issue 8, Pages 1596-1605, ISSN 0025-326X, https://doi.org/10.1016/j.marpolbul.2011.05.030.

Atmosphere Products. Appl. Opt. 2001, 40, 4790-4798.

Baekeland L. H. 1909. The Synthesis, Constitution, and Uses of Bakelite. Journal of Industrial & Engineering Chemistry. 1 (3), 149-161

Baini, M., Fossi, M. C., Galli, M., Caliani, I., Campani, T., Finoia, M. G., & Panti, C. (2018). Abundance and characterization of microplastics in the coastal waters of Tuscany (Italy): The application of the MSFD monitoring protocol in the Mediterranean Sea. Marine Pollution Bulletin, 133, 543–552. doi:10.1016/j.marpolbul.2018.06.016

Ballerini, T., Le Pen, J.-R., Andrady, A., Cole, M., Galgani, F., Kedzierski, M., Pedrotti, M.L.,ter halle, A., Van Arkel, K., Zettler, E., Amaral-Zettler, L., Bruzaud, S., Brandon, J., Durand, G., Enevoldsen, E., Eriksen, M., Fabre, P., Fossi, M.-C., Frère, L., Wong-WhaChung, P., 2018. Plastic pollution in the ocean: what we know and what we don't know about. Plast. Ocean Platf. – Camp 29. https://doi.org/10.13140/RG.2.2.36720.92160

Bannert, D., Kühn, F., and Ho¨rig, B., 1994, Ergebnissse spektroradiometrischer Untersuchungen an ölschieferaufschlüssen in Pakistan. 14. Wissenschaftlich-Technische Jahrestagung der DGPF vom 5–10 Oktober 1994 in Dresden, pp. 171–178.

Barnes, D. K. A., Galgani, F., Thompson, R. C., & Barlaz, M. (2009). Accumulation and fragmentation of plastic debris in global environments. Philosophical Transactions of the Royal Society B: Biological Sciences, 364(1526), 1985–1998. doi:10.1098/rstb.2008.0205

Brignac, K. C., Jung, M. R., King, C., Royer, S.-J., Blickley, L., Lamson, M. R., … Lynch, J. M. (2019). Marine Debris Polymers on Main Hawaiian Island Beaches, Sea Surface, and Seafloor. Environmental Science & Technology. doi:10.1021/acs.est.9b03561

Brown S, Nicholls R, Woodroffe C, Hanson S, Hinkel J, Kebede AS, et al. Sea-Level Rise Impacts and Responses: A Global Perspective In: Finkl CW, editor. Coastal Hazards. Netherlands: Springer; 2013. pp. 117–149.

C.J. Moore, S.L. Moore, M.K. Leecaster, S.B. Weisberg A comparison of plastic and plankton in the North Pacific central gyre Mar. Pollut. Bull., 42 (2001), pp. 1297-1300

Carolyn J. Foley, Zachary S. Feiner, Timothy D. Malinich, Tomas O. Höök, A meta-analysis of the effects of exposure to microplastics on fish and aquatic invertebrates, Science of The Total Environment, Volumes 631–632, 2018, Pages 550-559, ISSN 0048-9697, https://doi.org/10.1016/j.scitotenv.2018.03.046.

CLOUTIS, E. A. (1989). Spectral Reflectance Properties of Hydrocarbons: Remote-Sensing Implications. Science, 245(4914), 165–168. doi:10.1126/science.245.4914.165

Cox, C., and W. Munk (1954a), Measurement Of The Roughness Of The Sea Surface From Photographs Of The Suns Glitter, J. Opt. Soc. Am., 44, 838–850.

Cózar A, Sanz-Martín M, Martí E, González-Gordillo JI, Ubeda B, et al. (2015) Plastic Accumulation in the Mediterranean Sea. PLOS ONE 10(4): e0121762. https://doi.org/10.1371/journal.pone.0121762

Cózar, A., Echevarría, F., González-Gordillo, J. I., Irigoien, X., Úbeda, B., Hernández-León, S., et al. (2014). Plastic debris in the open ocean. Proc. Natl. Acad. Sci. U.S.A. 111, 10238–10244. doi: 10.1073/pnas.1314705111

Derek R. Peddle, H. Peter White, Raymond J. Soffer, John R. Miller, Ellsworth F. LeDrew, Reflectance processing of remote sensing spectroradiometer data, Computers & Geosciences, Volume 27, Issue 2, 2001, Pages 203-213, ISSN 0098-3004, https://doi.org/10.1016/S0098-3004(00)00096-0.

Diogo Neves, Paula Sobral, Joana Lia Ferreira, Tânia Pereira, Ingestion of microplastics by commercial fish off the Portuguese coast, Marine Pollution Bulletin, Volume 101, Issue 1, 2015, Pages 119-126, ISSN 0025-326X, https://doi.org/10.1016/j.marpolbul.2015.11.008.

Directionality of the Earth's Reflectances: A Comparison Study. Appl. Opt. 2002, 41, 974-990.

Durán-Alarcón, C., Santamaría-Artigas, A., Valenzuela, N., Mattar, C., 2014. RSR Calculator, una herramienta para el proceso de calibración/validación. In: Revista Española de Teledetección. 42. pp. 111–117.

European Space Agency (2015) Sentinel-2 MSI User Handbook, downloaded from: https://sentinels.copernicus.eu/documents/247904/685211/Sentinel-2_User_Handbook

F. Kühn, K. Oppermann & B. Hörig (2004) Hydrocarbon Index – an algorithm for hyperspectral detection of hydrocarbons , International Journal of Remote Sensing, 25:12, 2467-2473, DOI: 10.1080/01431160310001642287

FAO. 2016.The State of World Fisheries and Aquaculture 2016.Contributing to food security and nutrition for all. Rome. 200 pp.

Féret, J.B., Asner, G.P., 2011. Spectroscopic classification of tropical forest species using radiative transfer modeling. Remote Sens. Environ. 115 (9), 2415–2422. https://doi.org/10.1016/j.rse.2011.05.004.

from the Japanese Ocean Color and Temperature Scanner and the French Polarization and

Gallo, F., Fossi, C., Weber, R., Santillo, D., Sousa, J., Ingram, I., … Romano, D. (2018). Marine litter plastics and microplastics and their toxic chemicals components: the need for urgent preventive measures. Environmental sciences Europe, 30(1), 13. doi:10.1186/s12302-018-0139-z

Garaba, S. P., & Dierssen, H. M. (2018). An airborne remote sensing case study of synthetic hydrocarbon detection using short wave infrared absorption features identified from marine-harvested macro- and microplastics. Remote Sensing of Environment, 205, 224–235. doi:10.1016/j.rse.2017.11.023

Garaba, S. P., Schulz, J., Wernand, M. R., & Zielinski, O. (2012). Sunglint Detection for Unmanned and Automated Platforms. Sensors, 12(9), 12545–12561. doi:10.3390/s120912545

GESAMP (2019). Guidelines or the Monitoring and Assessment of Plastic Litter and Microplastics in the Ocean, eds P. J. Kershaw, A. Turra, and F. Galgani, Rep. Stud. GESAMP No. 99 (IMO/FAO/UNESCOIOC/UNIDO/WMO/IAEA/UN/UNEP/UNDP/ISA Joint Group of Experts on the Scientific Aspects of Marine Environmental Protection).

Geyer, Roland & Jambeck, Jenna & Law, Kara. (2017). Production, use, and fate of all plastics ever made. Science Advances. 3. e1700782. 10.1126/sciadv.1700782.

Gold, M., Mika, K., Horowitz, C., Herzog, M., & Leitner, L. (2013). Stemming the Tide of Plastic Marine Litter: A Global Action Agenda. UCLA: Emmett Institute on Climate Change and the Environment. Retrieved from https://escholarship.org/uc/item/6j74k1j3

Goldstein MC, Goodwin DS. 2013. Gooseneck barnacles (Lepas spp.) ingest microplastic debris in the North Pacific Subtropical Gyre. PeerJ 1:e184 https://doi.org/10.7717/peerj.184

Gordon, H.R., Brown, O.B., Jacobs, M.M., 1975. Computed relationships between the inherent and apparent optical properties of a flat homogeneous ocean. Appl. Opt. 14, 417–427.

Hammer, J., Kraak, M. H. S., & Parsons, J. R. (2012). Plastics in the Marine Environment: The Dark Side of a Modern Gift. Reviews of Environmental Contamination and Toxicology, 1–44. doi:10.1007/978-1-4614-3414-6_1

Harmel, T., and M. Chami (2013), Estimation of the sunglint radiance field from optical satellite imagery over open ocean: multidirectional approach and polarization aspects, J. Geophys. Res., 118, doi:10.1029/2012JC008221.

Harmel, T., Chami, M., Tormos, T., Reynaud, N., & Danis, P.-A. (2018). Sunglint correction of the Multi-Spectral Instrument (MSI)-SENTINEL-2 imagery over inland and sea waters from SWIR bands. Remote Sensing of Environment, 204, 308–321. doi:10.1016/j.rse.2017.10.022

Harmel, T., Chami, M., Tormos, T., Reynaud, N., & Danis, P.-A. (2018). Sunglint correction of the Multi-Spectral Instrument (MSI)-SENTINEL-2 imagery over inland and sea waters from SWIR bands. Remote Sensing of Environment, 204, 308–321. doi:10.1016/j.rse.2017.10.022

Hedley, J. D., Harborne, A. R., & Mumby, P. J. (2005). Technical note: Simple and robust removal of sun glint for mapping shallow-water benthos. International Journal of Remote Sensing, 26(10), 2107–2112. doi:10.1080/01431160500034086

Hochberg, E. J., Andrefouet, S., & Tyler, M. R. (2003). Sea surface correction of high spatial resolution ikonos images to improve bottom mapping in near-shore environments. IEEE Transactions on Geoscience and Remote Sensing, 41(7), 1724–1729. doi:10.1109/tgrs.2003.815408

Hörig, B., Kühn, F., Oschütz, F., & Lehmann, F. (2001). HyMap hyperspectral remote sensing to detect hydrocarbons. International Journal of Remote Sensing, 22(8), 1413–1422. doi:10.1080/01431160120909

http://gsp.humboldt.edu/olm_2016/courses/GSP_216_Online/lesson2-1/atmosphere.html

http://olympus.magnet.fsu.edu/primer/java/reflection/specular/index.html [Accessed: 17-10-2019]

https://vdrs.com/staging/tomra-optical-sorting/ Accessed: 16/10/2019

Hu, C., X. Li, W. G. Pichel, and F. E. Muller-Karger (2009), Detection of natural oil slicks in the NW Gulf of Mexico using MODIS imagery, Geophys. Res. Lett, 36, L01604.

HUETE, A. R. (2004). REMOTE SENSING FOR ENVIRONMENTAL MONITORING. Environmental Monitoring and Characterization, 183–206. doi:10.1016/b978-012064477-3/50013-8

Hulburt, E. O. (1934), Polarization of light at sea, J. Opt. Soc. Am., 24, 35–42.

Hwang Lee, Won Joon Shim, Jung-Hwan Kwon, Sorption capacity of plastic debris for hydrophobic organic chemicals, Science of The Total Environment, Volumes 470–471, 2014, Pages 1545-1552, ISSN 0048-9697, https://doi.org/10.1016/j.scitotenv.2013.08.023.

J. Mansui, A. Molcard, Y. Ourmières, Modelling the transport and accumulation of floating marine debris in the Mediterranean basin, Marine Pollution Bulletin, Volume 91, Issue 1, 2015, Pages 249-257, ISSN 0025-326X, https://doi.org/10.1016/j.marpolbul.2014.11.037.

Jambeck, Jenna & Geyer, Roland & Wilcox, Chris & Siegler, Theodore & Perryman, Miriam & Andrady, Anthony & Narayan, Ramani & Law, Kara. (2015). Marine pollution. Plastic waste inputs from land into the ocean. Science (New York, N.Y.). 347. 768-771. 10.1126/science.1260352.

Jerlov, N.G., 1968. Optical Oceanography. Elsevier Publishing Company, Amsterdam.

Kako S, Isobe A, Kataoka T, Hinata H. (2014) A decadal prediction of the quantity of plastic marine debris littered on beaches of the East Asian marginal seas, Marine Pollution Bulletin, Volume 81, Issue 1, Pages 174-184, ISSN 0025-326X, https://doi.org/10.1016/j.marpolbul.2014.01.057.

Karlsson, T. M., Grahn, H., van Bavel, B., & Geladi, P. (2016). Hyperspectral Imaging and Data Analysis for Detecting and Determining Plastic Contamination in Seawater Filtrates. Journal of Near Infrared Spectroscopy, 24(2), 141–149. doi:10.1255/jnirs.1212

Katja Dörnhöfer, Natascha Oppelt, Remote sensing for lake research and monitoring – Recent advances, Ecological Indicators, Volume 64, 2016, Pages 105-122, ISSN 1470-160X, https://doi.org/10.1016/j.ecolind.2015.12.009.

Kay Critchell, Jonathan Lambrechts, Modelling accumulation of marine plastics in the coastal zone; what are the dominant physical processes?, Estuarine, Coastal and Shelf Science, Volume 171, 2016, Pages 111-122, ISSN 0272-7714, https://doi.org/10.1016/j.ecss.2016.01.036.

Kay, S., Hedley, J., & Lavender, S. (2009). Sun Glint Correction of High and Low Spatial Resolution Images of Aquatic Scenes: a Review of Methods for Visible and Near-Infrared Wavelengths. Remote Sensing, 1(4), 697–730. doi:10.3390/rs1040697

Kokaly, R.F., Clark, R.N., Swayze, G.A., Livo, K.E., Hoefen, T.M., Pearson, N.C., Wise, R.A., Benzel, W.M., Lowers, H.A., Driscoll, R.L., and Klein, A.J., 2017, USGS Spectral Library Version 7: U.S. Geological Survey Data Series 1035, 61 p., https://doi.org/10.3133/ds1035.

Kooi, M., Nes, E., Scheffer, M., & Koelmans, A. A. (2017). Ups and Downs in the Ocean: Effects of Biofouling on Vertical Transport of Microplastics. Environmental science & technology, 51(14), 7963–7971. doi:10.1021/acs.est.6b04702

Kremezi M. and Karathanassi V. (2019) Correcting the BRDF effects on Sentinel-2 Ocean Images. Proceedings Volume 11174, Seventh International Conference on Remote Sensing and Geoinformation of the Environment (RSCy2019); 111741C (2019) https://doi.org/10.1117/12.2533653

Kühn F. and Hörig B. (1995) Environmental remote sensing for military exercise places. Remote Sensing and GIS for Site Characterizations: Applications and Standards, ASTM STP 1279, American Society for Testing and Materials, pp. 5–16.

L.C.-M. Lebreton, S.D. Greer, J.C. Borrero, Numerical modelling of floating debris in the world's oceans, Marine Pollution Bulletin, Volume 64, Issue 3, 2012, Pages 653-661, ISSN 0025-326X, https://doi.org/10.1016/j.marpolbul.2011.10.027.

Lavender, S.; Pinkerton, M.; Moore, G.; Aiken, J.; Blondeau-Patissier, D. Modification to the Atmospheric Correction of SeaWiFS Ocean Colour Images Over Turbid Waters. Cont. Shelf Res. 2005, 25, 539-555

Law, K. L., Moret-Ferguson, S., Maximenko, N. A., Proskurowski, G., Peacock, E. E., Hafner, J., & Reddy, C. M. (2010). Plastic Accumulation in the North Atlantic Subtropical Gyre. Science, 329(5996), 1185–1188. doi:10.1126/science.1192321

Lebreton L, Slat B, Ferrari F, Sainte-Rose B, Aitken J, Marthouse R, Hajbane S, Cunsolo S, Schwarz A, Levivier A, Noble K, Debeljak P, Maral H, Schoeneich-Argent R, Brambini R, Reisser J, (2018) Evidence that the Great Pacific Garbage Patch is rapidly accumulating plastic. Scientific Reports 4666

Lebreton L, van der Zwet J.D, Jan-Willem S, Boyan A, Reisser J. (2017) River plastic emissions to the world's oceans Nature Communications 15611 8 1

Luke A. Holmes, Andrew Turner, Richard C. Thompson, Adsorption of trace metals to plastic resin pellets in the marine environment, Environmental Pollution, Volume 160, 2012, Pages 42-48, ISSN 0269-7491, https://doi.org/10.1016/j.envpol.2011.08.052.

Lusher A, Hollman P, Mendoza-Hill J (2017) Microplastics in fisheries and aquaculture. Status of knowledge on their occurrence and implications for aquatic organisms and food safety. FAO Fisheries and Aquaculture Technical Paper, p 615

Matsuoka T, Nakashima T, Nagasawa N. 2005. A review of ghost fishing: scientific approaches to evaluation and solutions. Fisheries Science 691

Maximenko N, Corradi P, Law KL, Van Sebille E, Garaba SP, Lampitt RS, Galgani F, Martinez Vicente V, Goddijn-Murphy L, Veiga JM, Thompson RC, Maes C, Moller D, Löscher CR, Addamo AM, Lamson MR, Centurioni LR, Posth NR, Lumpkin R, Vinci M, Martins AM, Pieper CD, Isobe A, Hanke G, Edwards M, Chubarenko IP, Rodriguez E, Aliani S, Arias M, Asner GP, Brosich A, Carlton JT, Chao Y, Cook A-M, Cundy AB, Galloway TS, Giorgetti A, Goni GJ, Guichoux Y, Haram LE, Hardesty BD, Holdsworth N, Lebreton L, Leslie HA, Macadam-Somer I, Mace T, Manuel M, Marsh R, Martinez E, Mayor DJ, Le Moigne M, Molina Jack ME, Mowlem MC, Obbard RW, Pabortsava K, Robberson B, Rotaru A-E, Ruiz GM, Spedicato MT, Thiel M, Turra A and Wilcox C (2019) Toward the Integrated Marine Debris Observing System. Front. Mar. Sci. 6:447. doi: 10.3389/fmars.2019.00447

McCoy, F.W., 1988. Floating megalitter in the eastern Mediterranean. Mar. Pollut. Bull. 19 (1), 25–28.

Moller, D., Chao, Y., & Maximenko, N. (2016). Remote sensing of marine debris. 2016 IEEE International Geoscience and Remote Sensing Symposium (IGARSS). doi:10.1109/igarss.2016.7731005

Moroni, M., Mei, A., Leonardi, A., Lupo, E., & Marca, F. (2015). PET and PVC Separation with Hyperspectral Imagery. Sensors, 15(1), 2205–2227. doi:10.3390/s150102205

Moy K, Neilson B, Chung A, Meadows A,Castrence M,Ambagis S and Davidson K. (2018) Mapping coastal marine debris using aerial imagery and spatial analysis, Marine Pollution Bulletin, Volume 132, Pages 52-59, ISSN 0025-326X, https://doi.org/10.1016/j.marpolbul.2017.11.045.

MSFD (2013). Marine Strategy Framework Directive GES Technical Group on Marine Litter. Guidance on Monitoring of Marine Litter in European Seas, Luxembourg. Available online at: https://mcc.jrc.ec.europa.eu/documents/201702074014.pdf

Munari, C., Scoponi, M., & Mistri, M. (2017). Plastic debris in the Mediterranean Sea: Types, occurrence and distribution along Adriatic shorelines. Waste Management, 67, 385–391. doi:10.1016/j.wasman.2017.05.020

N. Maximenko, J. Hafner, P. Niiler Pathways of marine debris derived from trajectories of Lagrangian drifters Mar. Pollut. Bull., 65 (2012), pp. 51-62

Nash A.D, Impacts of marine debris on subsistence fishermen An exploratory study, Marine Pollution Bulletin, Volume 24, Issue 3, 1992, Pages 150-156, ISSN 0025-326X, https://doi.org/10.1016/0025-326X(92)90243-Y.

Nicola J. Beaumont, Margrethe Aanesen, Melanie C. Austen, Tobias Börger, James R. Clark, Matthew Cole, Tara Hooper, Penelope K. Lindeque, Christine Pascoe, Kayleigh J. Wyles, Global ecological, social and economic impacts of marine plastic, Marine Pollution Bulletin, Volume 142, 2019, Pages 189-195, ISSN 0025-326X, https://doi.org/10.1016/j.marpolbul.2019.03.022.

OECD 2018. Improving Plastics Management: Trends, policy responses, and the role of international co-operation and trade. OECD Environment Policy Paper No. 12, 3

of Sunglint for Accurate Prediction of Remotely Sensed Radiances. J. Quant. Spectrosc. Radiat.

Onjira, Pauline. (2014). Application of Remote sensing and Rainfall-Run-off Inundation Modeling to Near-Real Time Flood Monitoring in Kenya. 10.13140/RG.2.1.1283.3046.

Ottaviani, M.; Spurr, R.; Stamnes, K.; Li, W.; Su, W.; Wiscombe, W. Improving the Description

Parkes, Alex. Journal of the Society of Arts; London Vol. 14, (Nov 17, 1865): 81.

Pasternak, G., Zviely, D., Ribic, C. A., Ariel, A., & Spanier, E. (2017). Sources, composition and spatial distribution of marine debris along the Mediterranean coast of Israel. Marine Pollution Bulletin, 114(2), 1036–1045. doi:10.1016/j.marpolbul.2016.11.023

Pedrotti ML, Petit S, Elineau A, Bruzaud S, Crebassa J-C, Dumontet B, et al. (2016) Changes in the Floating Plastic Pollution of the Mediterranean Sea in Relation to the Distance to Land. PLoS ONE 11(8): e0161581. doi:10.1371/journal.pone.0161581

Plastics Europe Market Research Group (PEMRG). 2019. Plastics – the Facts 2018 An analysis of European plastics production, demand and waste data. https://www.plasticseurope.org/application/files/6315/4510/9658/Plastics_the_facts_2018_AF_web.pdf

Qiqing Chen, Annika Allgeier, Daqiang Yin, Henner Hollert, Leaching of endocrine disrupting chemicals from marine microplastics and mesoplastics under common life stress conditions, Environment International, Volume 130, 2019, 104938, ISSN 0160-4120, https://doi.org/10.1016/j.envint.2019.104938.

Raúl Aguirre Gómez, Spectral Reflectance Analysis of the Caribbean Sea, Geofísica Internacional, Volume 53, Issue 4, 2014, Pages 385-398, ISSN 0016-7169, https://doi.org/10.1016/S0016-7169(14)70073-X.

Serranti, S., Gargiulo, A., & Bonifazi, G. (2012). Hyperspectral imaging for process and quality control in recycling plants of polyolefin flakes. Journal of Near Infrared Spectroscopy, 20(5), 573. doi:10.1255/jnirs.1016

Serranti, S., Palmieri, R., Bonifazi, G., & Cózar, A. (2018). Characterization of microplastic litter from oceans by an innovative approach based on hyperspectral imaging. Waste Management, 76, 117–125. doi:10.1016/j.wasman.2018.03.003

Siegel, D.A.; Wang, M.; Maritorena, S.; Robinson, W. Atmospheric Correction of Satellite Ocean Color Imagery: The Black Pixel Assumption. Appl. Opt. 2000, 39, 3582-3591.

Suaria, G., & Aliani, S. (2014). Floating debris in the Mediterranean Sea. Marine Pollution Bulletin, 86(1-2), 494–504. doi:10.1016/j.marpolbul.2014.06.025

Suaria, G., Avio, C. G., Mineo, A., Lattin, G. L., Magaldi, M. G., Belmonte, G. Aliani, S. (2016). The Mediterranean Plastic Soup: synthetic polymers in Mediterranean surface waters. Scientific Reports, 6(1). doi:10.1038/srep37551

Suaria, G., Melinte-Dobrinescu, M. C., Ion, G., & Aliani, S. (2015). First observations on the abundance and composition of floating debris in the North-western Black Sea. Marine Environmental Research, 107, 45–49. doi:10.1016/j.marenvres.2015.03.011

Thevenon, F., Carroll C., Sousa J. (editors), 2014. Plastic Debris in the Ocean: The Characterization of Marine Plastics and their Environmental Impacts, Situation Analysis Report. Gland, Switzerland: IUCN. 52 pp

Thompson Richard C., Moore Charles J., vom Saal Frederick S. and Swan Shanna H. (2009) Plastics, the environment and human health: current consensus and future trends364Phil. Trans. R. Soc. B

Tokiwa Y, Calabia BP, Ugwu CU, Aiba S. 2009. Biodegradability of Plastics. International Journal of Molecular Sciences.; 10(9):3722-3742.

Topcu, E.N., Tonay, A.M., Öztürk, B., 2010. A preliminary study on marine litter in the Aegean Sea. Rapp. Comm. int. Mer Médit 39, 804.

Transf. 2008, 109, 2364-2375.

Ulrici, A., Serranti, S., Ferrari, C., Cesare, D., Foca, G., & Bonifazi, G. (2013). Efficient chemometric strategies for PET–PLA discrimination in recycling plants using hyperspectral imaging. Chemometrics and Intelligent Laboratory Systems, 122, 31–39. doi:10.1016/j.chemolab.2013.01.001

UNEP/MAP (2015) Marine Litter Assessment in the Mediterranean

UNEP/MAP/MEDPOL, 2009. Results of the Assessment of the Status of Marine Litter in the Mediterranean. Meeting of MED POL Focal Points No. 334, 91 pp.

Van Sebille E, Wilcox C, Lebreton L, Maximenko N, Hardesty B, Van Franeker J, Eriksen M, Siegel D, Galgani F, & Law Kara. (2015). A global inventory of small floating plastic debris. Environmental Research Letters. 10. 124006. 10.1088/1748-9326/10/12/124006.

Vanhellemont, Q. (2019). Adaptation of the dark spectrum fitting atmospheric correction for aquatic applications of the Landsat and Sentinel-2 archives. Remote Sensing of Environment, 225, 175–192. doi:10.1016/j.rse.2019.03.010

Vázquez-Guardado, A., Money, M., McKinney, N., & Chanda, D. (2015). Multi-spectral infrared spectroscopy for robust plastic identification. Applied Optics, 54(24), 7396. doi:10.1364/ao.54.007396

Vázquez-Guardado, A., Money, M., McKinney, N., & Chanda, D. (2015). Multi-spectral infrared spectroscopy for robust plastic identification. Applied Optics, 54(24), 7396. doi:10.1364/ao.54.007396

Veenstra, T. S., & Churnside, J. H. (2012). Airborne sensors for detecting large marine debris at sea. Marine Pollution Bulletin, 65(1-3), 63–68. doi:10.1016/j.marpolbul.2010.11.018

Wang, M.; Bailey, S. Correction of Sun Glint Contamination on the SeaWiFS Ocean and

Wang, M.; Isaacman, A.; Franz, B.; McClain, C. Ocean-Color Optical Property Data Derived

Wong, C. S., Green, D. R. & Cretney, W. J. (1974) Quantitative tar and plastic waste distributions in the Pacific Ocean. Nature 247, 30–32.

Wright, S. L., & Kelly, F. J. (2017). Plastic and Human Health: A Micro Issue? Environmental Science & Technology, 51(12), 6634–6647. doi:10.1021/acs.est.7b00423

Ziccardi, L. M., Edgington, A. , Hentz, K. , Kulacki, K. J. and Kane Driscoll, S. (2016), Microplastics as vectors for bioaccumulation of hydrophobic organic chemicals in the marine environment: A state-of-the-science review. Environ Toxicol Chem, 35: 1667-1676. doi:10.1002/etc.3461

Appendices

Appendix 1: Litter types as per UNEP/IOC (2009)

Number	Material	Code	Litter type
1	Plastic	PL01	Bottle caps & lids
2	Plastic	PL02	Bottles < 2 L
3	Plastic	PL03	Bottles, drums, jerrycans & buckets > 2 L
4	Plastic	PL04	Knives, forks, spoons, straws, stirrers, (cutlery)
5	Plastic	PL05	Drink package rings, six-pack rings, ring carriers
6	Plastic	PL06	Food containers (fast food, cups, lunch boxes & similar)
7	Plastic	PL07	Plastic bags (opaque & clear)
8	Plastic	PL08	Toys & party poppers
9	Plastic	PL09	Gloves
10	Plastic	PL10	Cigarette lighters
11	Plastic	PL11	Cigarettes, butts & filters
12	Plastic	PL12	Syringes
13	Plastic	PL13	Baskets, crates & trays
14	Plastic	PL14	Plastic buoys
15	Plastic	PL15	Mesh bags (vegetable, oyster nets & mussel bags)
16	Plastic	PL16	Sheeting (tarpaulin or other woven plastic bags, palette wrap)
17	Plastic	PL17	Fishing gear (lures, traps & pots)
18	Plastic	PL18	Monofilament line
19	Plastic	PL19	Rope
20	Plastic	PL20	Fishing net
21	Plastic	PL21	Strapping
22	Plastic	PL22	Fibreglass fragments
23	Plastic	PL23	Resin pellets
24	Plastic	PL24	Other (specify)
25	Foamed Plastic	FP01	Foam sponge
26	Foamed Plastic	FP02	Cups & food packs
27	Foamed Plastic	FP03	Foam buoys
28	Foamed Plastic	FP04	Foam (insulation & packaging)
29	Foamed Plastic	FP05	Other (specify)
30	Cloth	CL01	Clothing, shoes, hats & towels
31	Cloth	CL02	Backpacks & bags
32	Cloth	CL03	Canvas, sailcloth & sacking (hessian)
33	Cloth	CL04	Rope & string
34	Cloth	CL05	Carpet & furnishing
35	Cloth	CL06	Other cloth (including rags)
36	Glass & ceramic	GC01	Construction material (brick, cement, pipes)

Number	Material	Code	Litter type
37	Glass & ceramic	GC02	Bottles & jars
38	Glass & ceramic	GC03	Tableware (plates & cups)
39	Glass & ceramic	GC04	Light globes/bulbs
40	Glass & ceramic	GC05	Fluorescent light tubes
41	Glass & ceramic	GC06	Glass buoys
42	Glass & ceramic	GC07	Glass or ceramic fragments
43	Glass & ceramic	GC08	Other (specify)
44	Metal	ME01	Tableware (plates, cups & cutlery)
45	Metal	ME02	Bottle caps, lids & pull tabs
46	Metal	ME03	Aluminium drink cans
47	Metal	ME04	Other cans (< 4 L)
48	Metal	ME05	Gas bottles, drums & buckets (> 4 L)
49	Metal	ME06	Foil wrappers
50	Metal	ME07	Fishing related (sinkers, lures, hooks, traps & pots)
51	Metal	ME08	Fragments
52	Metal	ME09	Wire, wire mesh & barbed wire
53	Metal	ME10	Other (specify), including appliances
54	Paper & cardboard	PC01	Paper (including newspapers & magazines)
55	Paper & cardboard	PC02	Cardboard boxes & fragments
56	Paper & cardboard	PC03	Cups, food trays, food wrappers, cigarette packs, drink containers
57	Paper & cardboard	PC04	Tubes for fireworks
58	Paper & cardboard	PC05	Other (specify)
59	Rubber	RB01	Balloons, balls & toys
60	Rubber	RB02	Footwear (flip-flops)
61	Rubber	RB03	Gloves
62	Rubber	RB04	Tyres
63	Rubber	RB05	Inner-tubes and rubber sheet
64	Rubber	RB06	Rubber bands
65	Rubber	RB07	Condoms
66	Rubber	RB08	Other (specify)
67	Wood	WD01	Corks
68	Wood	WD02	Fishing traps and pots
69	Wood	WD03	Ice-cream sticks, chip forks, chopsticks & toothpicks
70	Wood	WD04	Processed timber and pallet crates
71	Wood	WD05	Matches & fireworks
72	Wood	WD06	Other (specify)
73	Other	OT01	Paraffin or wax
74	Other	OT02	Sanitary (nappies, cotton buds, tampon applicators, toothbrushes)
75	Other	OT03	Appliances & Electronics
76	Other	OT04	Batteries (torch type)
77	Other	OT05	Other (specify)

General litter class	Code	Litter description with examples
Containers	RL01	Bottle caps, lids & pull tabs
	RL02	Bottles < 2 L
	RL03	Bottles, drums & buckets > 2 L
Fishing & Boating	RL04	Buoys
	RL05	Fishing net
	RL06	Fishing related (sinkers, lures, hooks, traps, pots & baskets/trays)
	RL07	Monofilament line
	RL08	Rope
Food & Beverage	RL09	Cups, food trays, fast food wrappers & cardboard drink containers
	RL10	Drink cans
	RL11	Drink package rings
	RL12	Ice-cream sticks, chip forks, chopsticks, toothpicks, matches & fireworks
Packaging	RL13	Foam (insulation & packaging)
	RL14	Paper & cardboard
	RL15	Plastic bags (opaque & clear)
	RL16	Plastic sheet or plastic tarpaulin
	RL17	Strapping
Sanitary	RL18	Sanitary (nappies, tampon applicators, cotton buds, condoms, etc)
Smoking	RL19	Cigarette butts
	RL20	Cigarette lighters
Other	RL21	Fluorescent light tubes
	RL22	Light globes
	RL23	Other (specify)
	RL24	Processed timber
	RL25	Rags, clothing, shoes, hats & towels
	RL26	Tableware
	RL27	Toys
	RL28	Tyres & Inner-tubes
	RL29	Wire, wire mesh & barbed wire

Appendix 2: collected marine debris sorting form

PLP2020 marine debris cataloguing form								
Date:			Start time:			End time:		
Beach of origin:								
Total weight (kg):								
Weight ≤ 5 cm (kg):								
Weight ≥ 10 cm (kg):								
No. of items ≥ 5 cm:								
No. of items ≥ 10 cm:								
Polymer composition ≥ 5 cm (number of items)								
PE	PP	PS	EPS	PET				unknown
Polymer composition ≥ 10 cm (number of items)								
PE	PP	PS	EPS	PET				unknown
Signed by:								

Appendix 3: litter strand inventory form

PLP 2020 small target litter strand inventory form				
Strand No.	Polymer type(s)	No. of items	Weight (kg)	Litter types used (UNEP/IOC, 2009 litter codes)

Appendix 4: team organization and filling forms.

Phase 1 - task teams and key people	
Beach cleanings	
Organiser:	1)
Field managers:	2)
	3)
Litter cataloguing	
Task managers:	1)
	2)
	3)
Construction team	
Team manager:	1)
Small targets lead:	2)
Large target lead:	3)
Team members:	4)
	5)
	6)
	7)
	8)
	9)
	10)

Phase 2 - task teams and key people	
Field managers:	1)
	2)
Beach team	
Team lead:	1)
Team members:	2)
	3)
	4)
	5)
	6)
Dive team	
Team lead:	1)
Team members:	2)
	3)
	4)
Drone team	
Team lead:	1)
Team members:	2)
	3)
Dinghy team	
Team lead:	1)
Team members:	2)
	3)
Data management	
Team members:	1)
	2)

Appendix 5

<table>
<tr><td colspan="8">PLP 2020 field report form - to be filled on site by a single individual throughout</td></tr>
<tr><td rowspan="2">Date:</td><td rowspan="2"></td><td colspan="6">Satellites:</td></tr>
<tr><td>Sentinel 2</td><td>Sentinel 1</td><td>Landsat 8</td><td>PRISMA</td><td>Wordview III</td><td>PlanetScope</td></tr>
<tr><td rowspan="2">Start time:</td><td rowspan="2"></td><td></td><td></td><td></td><td></td><td></td><td></td></tr>
<tr><td colspan="6" rowspan="2">Remarks:</td></tr>
<tr><td rowspan="2">Atm.conditions:</td><td rowspan="2"></td></tr>
<tr><td colspan="3">UAS:</td><td colspan="3">Remarks:</td></tr>
<tr><td rowspan="2">Sea state:</td><td rowspan="2"></td><td>RGB</td><td>lift-off</td><td>touch-down</td><td colspan="3" rowspan="6"></td></tr>
<tr><td></td><td></td><td></td></tr>
<tr><td rowspan="2">Wind speed (m/s) @ start:</td><td rowspan="2"></td><td>slnt-multi</td><td>lift-off</td><td>touch-down</td></tr>
<tr><td></td><td></td><td></td></tr>
<tr><td rowspan="2">End time:</td><td rowspan="2"></td><td>hyper</td><td>lift-off</td><td>touch-down</td></tr>
<tr><td></td><td></td><td></td></tr>
<tr><td>Target configuration and % coverage:</td><td colspan="7"></td></tr>
<tr><td>General remarks:</td><td colspan="7"></td></tr>
<tr><td>Filled by:</td><td colspan="7"></td></tr>
</table>